R. & M. No. 3404

MINISTRY OF AVIATION

AERONAUTICAL RESEARCH COUNCIL
REPORTS AND MEMORANDA

Mechanical Aspects of Turbine Blade Cooling

Part I.—Description of an Experimental High-Temperature Turbine and Associated Test Rig (Cooled Turbine No. 126)

By N. E. WALDREN and J. A. FLINT

Part II.—The Behaviour of Extruded Air-Cooled Rotor Blades Subjected to Steady High Temperature and Rotational Speed

By J. F. BARNES, J. E. NORTHWOOD and D. E. FRAY

LONDON: HER MAJESTY'S STATIONERY OFFICE
1965
PRICE £1 2s. 0d. NET

Mechanical Aspects of Turbine Blade Cooling

COMMUNICATED BY THE DEPUTY CONTROLLER AIRCRAFT (RESEARCH AND DEVELOPMENT), MINISTRY OF AVIATION

*Reports and Memoranda No. 3404**

December, 1962

Part I.—Description of an Experimental High-Temperature Turbine and Associated Test Rig (Cooled Turbine No. 126)

By N. E. WALDREN and J. A. FLINT

Summary.

Part I of this report describes an experimental, cooled turbine, designed and built for research into problems associated with the operation of turbines at very high gas temperatures, in particular, the problem of turbine blade cooling.

The turbine structure and the associated test rig have been designed to permit testing of turbine blades over a wide range of turbine entry gas temperature from 900°K to 1600°K and entry gas pressure from $\frac{2}{3}$ to 5 atmospheres giving a wide range of gas-flow Reynolds numbers to the blades.

A further aim of the design has been to achieve rapid access to blades under test and to allow the testing of a moderately wide variety of both blades and cooling systems with relatively minor alteration to the turbine or test rig.

Initial proving tests have been made to observe the mechanical behaviour of the turbine and test rig and to establish optimum coolant quantities required to cool the turbine structure.

Following minor alterations and adjustments satisfactory performance was achieved over the major portion of the design speed range while operating at moderate gas temperatures, from 900°K to 1100°K (atmospheric turbine exhaust). Results suggest that the turbine structure should be sufficiently well cooled to permit the testing of blades over the full range of turbine inlet gas temperature envisaged.

LIST OF CONTENTS

* Part I replaces N.G.T.E. Report No. R.237—A.R.C. 21 504.
Part II replaces N.G.T.E. Report No. R.251—A.R.C. 24 567.

LIST OF APPENDICES

LIST OF ILLUSTRATIONS

---

1. *Introduction.*

An experimental turbine, designated the No. 126 cooled turbine, has been designed and built with the object of furthering the research into problems associated with the operation of turbines at very high gas temperatures, in particular, the problem of turbine blade cooling.

A great deal of experience has been gained from tests carried out on an earlier high-temperature, air-cooled turbine described in Ref. 1, and the results of this work have served to emphasize the value of testing cooled blades under realistic conditions of gas flow, temperature and stress. However, during the course of these tests it became apparent that a number of major improvements in test-rig design were desirable to achieve greater flexibility in use, and every effort has been made to incorporate such improvements in the new turbine and test rig. The following report gives a brief description of the No. 126 cooled turbine and the associated test rig.

2. *Basic Scantlings.*

For reasons of economy it was considered desirable to limit the turbine size to a mininum necessary for general research purposes. A controlling feature was the minimum convenient size of blading. Experience has demonstrated that the fabrication of air-cooled blades having good cooling characteristics and permitting comprehensive installation of buried thermocouples becomes very difficult when the blade chord is less than about $1\frac{1}{2}$ in. At the same time, large blade lengths, coupled with moderately large values of turbine hub ratio, can result in turbines having gas swallowing capacities and power outputs which are inconveniently large for a general-purpose research rig. The cost of the associated plant (air compressor, power absorption dynamometer, etc.) also becomes excessive. The basic scantlings for the present turbine were decided eventually as:

Blade chord	$1\frac{1}{2}$ to $2\frac{1}{4}$ in.
Blade height	3 in.
Blade-tip diameter	19 in.
Hub diameter	13 in.
Hub ratio	0·685
Maximum blade-tip speed	1100 ft/sec
Maximum rotational speed	13 300 rev/min
Maximum power output	3000 h.p.
Turbine inlet gas temperature	900°K to 1600°K
Turbine stage pressure ratio	1·05 to 2·0
Turbine inlet gas pressure	5 atm. to $\frac{2}{3}$ atm.

The moderately high range of turbine inlet pressure was introduced in order to permit testing over a wide range of gas-flow Reynolds numbers. Earlier work has indicated that Reynolds number may be a significant parameter controlling the performance of air-cooled turbine blades, particularly when low values of Reynolds number (less than 1×10^5) are encountered.

The first assembly of the turbine conforms to these scantlings. It will be appreciated, however, from the later description of the construction that some of these scantlings (such as blade size and hub ratio) might be adjusted to some extent without major alteration in the basic structural design.

A plant compressor delivering up to 60 lb/sec of air at 6/1 pressure ratio is available for driving the turbine when testing with exhaust pressures higher than atmospheric. For sub-atmospheric pressure testing the same air supply may be used to drive an ejector situated in the exhaust ducting from the turbine.

3. *Basic Structural Requirements.*

Certain major features are desirable in a turbine test-rig design to meet the aforementioned requirements. These may be enumerated as follows:

(i) rapid and simple partial dismantling to provide access to blades and discs,

(ii) versatility in use,

(iii) versatility in the form of combustion system applied to the test rig.

Since the rig is intended primarily for blade research it is only necessary that the blades, and turbine annulus in the immediate vicinity of the blades, be cooled in a manner representative of

possible engine design. The external turbine structure, ducting, etc. are essential rig components from which reliability and long life are demanded. These have been treated as such in the present test rig, no attempt being made to make the rig structure (excluding blading) representative of, say, typical aircraft engine practice. In such components free use has been made of water cooling to achieve a very safe and conservative mechanical structure.

4. *Description of Turbine and Associated Test Rig.*

A general view of the turbine and test rig is given in Fig. 1 and the principal features of the rig are indicated in Fig. 2.

The turbine, together with a high-speed water brake, is mounted on a large fabricated steel bedplate. The brake is directly coupled to the turbine and has the combined duty of both absorbing turbine power and measuring shaft torque in conjunction with a sensitive weigh gear and, in this latter respect, is supported in air bearings to obtain the best possible accuracy in measurement. Attached to the brake shaft is a carbon-brush-type slip-ring unit, used in the measurement of rotor-blade temperature, an overspeed centrifugal switch and a turbine speed tachometer. A single, large combustion chamber, burning a premixed stream of vaporized kerosine and compressed air, produces the high-temperature gases on which the turbine operates.

The hot exhaust gases are discharged into four cylindrical ducts, each of identical shape and symmetrically disposed around the exhaust to ensure equal pressure losses and uniform circumferential flow distribution upstream, in the turbine annulus. The ducts sweep radially outwards from the turbine centre line to allow the water brake to be positioned close to the turbine exhaust with the minimum length of interconnecting shafting, a necessary feature to avoid shaft whirling within the operating speed range. A large steel framework supports the four exhaust ducts and carries the pressure load exerted by exhaust restrictor plates when fitted for turbine operation at high gas densities.

Further compressed air is individually metered to the various cooled regions in the turbine. Referring to Fig. 3 these cooled regions are:

(a) turbine outer diameter
  (i) liner at inlet to nozzle row
  (ii) nozzle blades
  (iii) rotor shroud
  (iv) exhaust liners and exhaust-gas diluent

(b) turbine inner diameter (air *via* cooler at 30°C)
  (i) (a) liner at inlet to nozzle row
    (b) nozzle shroud
  (ii) rotor disc, inlet face and rotor blade roots
  (iii) rotor blades (*via* turbine hollow shaft and discs)
  (iv) rotor disc, exhaust face.

For the purpose of inspection or modification the turbine may be conveniently broken down into five sub-assemblies (Fig. 8a) each assembly being complete with instrumentation and coolant pipework. These sub-assemblies are:

(i) turbine inlet assembly

(ii) nozzle blade and housing assembly

(iii) rotor blade, disc and shaft assembly

(iv) rotor shroud assembly

(v) turbine exhaust assembly.

The exhaust assembly forms the major part of the turbine and, as indicated in Fig. 3, is constructed mainly in SG iron and cooled with water. On this large assembly depends the alignment of both shafting and ducting. The four remaining assemblies are supported by the exhaust assembly and it is possible to remove them without disturbing the major portion of the test rig. This feature is illustrated in Fig. 1 in which the turbine inlet and nozzle assemblies have been removed to give access to the blading.

The inlet assembly, *see* Fig. 4, is directly connected to the combustion chamber and forms the entry to the turbine nozzle annulus. It has been constructed entirely in sheet metal in a manner similar in principle to the combustion chamber, *see* Fig. 5, in which liners, guiding the hot gases to the turbine, are cooled by radiating heat to adjacent water jackets. The jackets withstand the full static-pressure load of the gas stream and the liners (Nimonic 75) are thus capable of safe operation at metal temperatures as high as 1000°C. The cooling influence of duct walls on the gas temperature distribution at entry to the turbine is thereby minimised.

The blading for the initial build of the turbine is shown in Fig. 6 and details are given in Appendix I. Nozzle blades have been formed by welding root blocks and tip shrouds to extrusions of aerofoil cross-section containing spanwise cooling passages. Cooling air flows radially inwards through these passages, spills into an annular space formed by the blade tip shrouds and finally discharges into the gas stream between nozzle and rotor blade row. Blades are shrouded to ensure uniform chordwise coolant flow as there will be a substantial gas-stream static-pressure drop across the nozzle row in this direction. Shrouds are also an essential pre-requisite to high turbine aerodynamic efficiency.

In forming a root fixing for the rotor blades the high stresses and temperatures to be encountered made it desirable that the use of either welding or brazing should be avoided. For this set of blades therefore, it was decided to extrude billets from which a root fixture could be machined as an integral part of the blade. To ease manufacture, separate wedge-shaped spacers were designed to mate with the blade concave surface and complete the root platform. These spacers are provided with axial slots to allow passage of cooling air through the roots as shown in Fig. 6.

The blades and spacers are clamped in circumferential grooves between twin rotor discs. Compared with the single disc with axial firtree root fixings the twin disc lends itself more readily to blade-cooling schemes, the coolant being introduced to the blade roots between the discs. However, it is possible to fit either type in the turbine.

The rotor shroud assembly has been designed to suit the first set of unshrouded rotor blades and is a separate unit to allow the removal of exhaust liners. It is, however, a relatively small assembly and a minor alteration is all that is required to accommodate blades with integral shrouds.

The exhaust annulus, fabricated in Nimonic 75 sheet metal, forms the transition from the annular passage, immediately after the turbine stage, to four equal, segmental outlets. The liners are perforated and the injection of a large quantity of cooling air (up to 50 per cent of the gas mass flow) serves the dual purpose of liner cooling and exhaust-gas dilution, the latter being necessary to lower the temperature of the very hot gases before discharging into the four uncooled Nimonic 90 exhaust ducts.

5. *Basic Instrumentation.*

In order to make a thorough investigation into the performance of a set of air-cooled turbine blades it is necessary to have a precise knowledge of the variables influencing:

(i) turbine overall performance

(ii) heat transfer from gas to blades

(iii) heat transfer from blades to coolant.

The following basic measurements are therefore required as illustrated in Figs. 7, 8a, 8b and 8c:

(a) total-head temperature (mean and distribution) at turbine inlet

(b) total-head and static pressures at turbine inlet and outlet

(c) turbine gas mass flow

(d) turbine rotational speed

(e) turbine power output

(f) blade-coolant mass flow

(g) blade-coolant temperature

(h) blade-coolant header pressure (at blade root)

(i) blade-metal temperature (Figs. 8b and 8c).

Further instrumentation is required to ensure that adequate cooling of the turbine structure is provided and Fig. 8a indicates the disposition of the large number of thermocouples around the turbine annulus together with the various cooling-air supplies.

Turbine inlet gas temperature, being an important datum for all test results, is carefully measured by means of sonic-suction pyrometers traversed across the inlet annulus. At gas temperatures higher than about 900°C, however, pyrometers and pitot combs will be removed from the inlet annulus to avoid possible failure and damage to blading. Under these conditions turbine inlet mean gas temperature will be estimated using a calibration of combustion efficiency (*see* Section 6) in conjunction with measured air and fuel flow. Inlet total-head pressure will be calculated from a calibration between $P_{\text{tot}}/P_{\text{stat}}$ and $W\sqrt{T}/P_{\text{stat}}$ (conditions at inlet to stage) obtained during tests at the lower gas temperatures[1].

The provision of thermocouples in the rotor blades presents a particularly difficult problem and, for this reason, Fig. 9 has been included to illustrate the method adopted for the first set of blades. Thermocouples are made by drawing down nickel sheaths, firmly, on to insulated thermocouple wire. The thermocouples are inserted into pockets machined in the blade surface and keyed in position by sprayed nickel. A junction, between the fine thermocouple wires and heavier leads to a slip-ring unit, is made on the inlet face of the disc using insulated dumb-bells in thermocouple material, 'Araldite' being used to maintain the insulation of the fine wires at the point where they leave the nickel sheaths. In the course of rig development a considerable amount of trouble was experienced with this junction at the rotor hub between the fine thermocouple wires in the rotor and heavier leads in the shaft. Extreme care is required to avoid breakdown of insulation or fracture of the fine wires under centrifugal load, and the arrangement described here was arrived at after some development. Throughout the system care is taken to ensure that thermocouples, junction and leads are adequately supported against centrifugal loading. A 25-pin plug between turbine and brake allows removal of the rotor shaft.

6. *Brief Account of Initial Operating Experience.*

While the turbine was in the course of construction, proving tests were carried out on the sheet-metal inlet assembly (Fig. 4) in conjunction with the combustion chamber and a major portion of the test rig. Tests covered a range of combustion delivery temperatures up to a maximum of 1500°K at delivery pressures of 1, 2 and 3 atm. Under these conditions a calibration of combustion efficiency by gas analysis was obtained for use in the future estimation of turbine inlet mean gas temperature at the higher level referred to in Section 5. At the conclusion of the tests the condition of both inlet assembly and combustion chamber was good, no overheating or distortion having taken place.

The installation of the turbine followed, the turbine being fitted with air-cooled nozzle blades and uncooled Nimonic 80A rotor blades as the air-cooled rotor blades were, at that time, in the early stages of manufacture. Ensuing tests were concentrated on proving the mechanical reliability of the rig as a whole, including the rotor thermocouple system, over the major part of the speed range and observing the cooling behaviour of the turbine structure over a limited range of gas temperature. Air-cooled rotor blades were then fitted and further testing carried out to confirm these results.

Throughout the test the mechanical behaviour of the turbine and test rig was satisfactory at speeds ranging up to 12 000 rev/min. From observations made while operating at turbine inlet gas temperatures between 900°K and 1100°K and with nominally atmospheric turbine exhaust pressure, it has been possible to make an approximate assessment of the individual quantities of cooling air required to achieve satisfactory life of the turbine structure at a gas temperature of 1600°K. These results have been tabulated in Appendix II and compare well with the structure temperatures assumed for the mechanical design on which mechanical clearances have been based.

In general an attempt has been made to minimise the necessary degree of cooling required for the turbine annulus in the vicinity of the blades in order to avoid any influence that the overcooling of these parts may have on blade-cooling results.* Some adjustments have been necessary to obtain a correct balance of cooling flow to the nozzle shroud where restrictors are used to divide the flow between upstream and downstream regions, this balance being influenced by the static-pressure drop across the nozzle blade row. Cooling flows to the upstream and downstream faces of the rotor disc have also been adjusted to maintain a small flow of cooling air into the gas stream between the blade rows and thereby avoid hot gases penetrating to the rotor blade roots.

7. *Conclusions.*

An experimental, cooled turbine has been designed and built, and initial proving tests have been made to observe the mechanical behaviour of the turbine and test rig and to establish optimum coolant quantities required to cool the turbine structure.

Following minor alterations and adjustments, the turbine and associated test rig performed satisfactorily over the major portion of the design speed range while operating at a moderate level of gas temperature. Some difficulty, however, was experienced with the rotor-blade thermocouple wiring before a reliable system was finally developed.

Test results suggest that the turbine structure should be sufficiently well cooled to permit the testing of blades over the full range of turbine inlet gas temperature, from 900°K to 1600°K.

---

* Overcooling of the turbine annulus may result in a significant degree of blade cooling due to heat radiation from hot blades to cool annulus. Although this is a legitimate means for cooling the blades it is desirable to avoid it in research testing where data are required on the effectiveness of convective cooling flow.

REFERENCES

No.	*Author(s)*	*Title, etc.*
1	D. G. Ainley, N. E. Waldren and K. Hughes.	Investigations on an experimental air-cooled turbine. Parts I and II. A.R.C. R. & M.2975. March, 1954.
2	P. Martin and E. L. Hartley . .	The development and testing of a combustion chamber for 1400°C outlet temperature and a temperature distribution better than 3 per cent. N.G.T.E. Memorandum M.248. November, 1955.

APPENDIX I

Nozzle and Rotor Blade Details (*Extruded Nimonic* 90)

All blades of constant section, untwisted

	Nozzle	*Rotor*
Number of blades in row	29	40
Blade height	3 in.	3 in.
Chord	2·25 in.	1·62 in.
Maximum thickness	0·425 in.	0·40 in.
Leading-edge radius	0·10 in.	0·115 in.
Trailing-edge radius	0·04 in.	0·033 in.
Mean diameter	16 in.	16 in.
Mean-diameter pitch	1·73 in.	1·255 in.
Mean-diameter blade opening	0·895 in.	0·749 in.
Stagger angle	36° 30′	22° 46′
Blade inlet angle	0°	15°
Blade outlet angle	58°	47° 30′
Blade tip clearance (mean)	Shrouded	0·060 in.
Moment of inertia of section I_{min} (parallel to chord)	0·008304 in^4	0·00487 in^4
Distance, chord to neutral axis	0·248 in.	0·239 in.
Moment of inertia of section I_{max} (normal to chord)	0·179312 in^4	0·05415 in^4
Distance, L.E. to neutral axis	1·004 in.	0·678 in.

APPENDIX II

Turbine Cooling-Air Supplies and Resulting Structure Temperatures

Cooling-air supplies			Turbine structure temperature—°C			
Cooled region	Quantity % of gas mass flow	Air temp. °C	Thermo-couple location Fig. 8a	$\frac{T_M - T_C}{T_G - T_C}$ 900°K to 1100°K gas temp.	Predicted* at 1600°K gas temp.	Design (mech.) at 1600°K gas temp.
1. Outer liner at inlet	0·3	100	N1	0·3	470	400
			N2	0·09	210	250
2. Nozzle blades	2·0	150	N3	0·32	530	500
			N4, N5, N6	Subject of later reports		
3. Rotor shroud (mid-stage)	0·5	100	N7	0·36	550	400
			N8	0·12	250	250
			RS1	0·58	810	800
			RS2	0·12	250	250
4. Exhaust liners and gas diluent	20 (up to 50%)	200	RS3	0·39	640	800
			E2	0·29	527	1000
5. Inner liner at inlet and nozzle shroud	0·5	20	N9	0·6	810	800
			N10	0·25	350	350
6. Rotor disc, blade roots and upstream members	0·5	20	N11	0·3	410	350
7. Rotor blades	1·0 to 1·5	20	R1, R2, R3, R4, R5, R6	Subject of later reports		
8. Rotor disc and down-stream members	0·5	20	E1	0·15	220	400
			E3	0·4	550	1000

Note 1. Thermocouples have been grouped and related to the cooling flow by which they have been mainly influenced.

*Note 2. Predicted structure temperatures (T_M) have been obtained by extrapolating the results of test with turbine inlet gas temperatures (T_G) ranging between 900°K and 1100°K using the approximate relation:

$$\frac{T_M - T_C}{T_G - T_C} = \text{Constant where } T_C = \text{cooling-air temperature.}$$

Note 3. All thermocouples have been duplicated in diametrically opposite locations in the turbine. The maximum of the two readings has been taken in all cases.

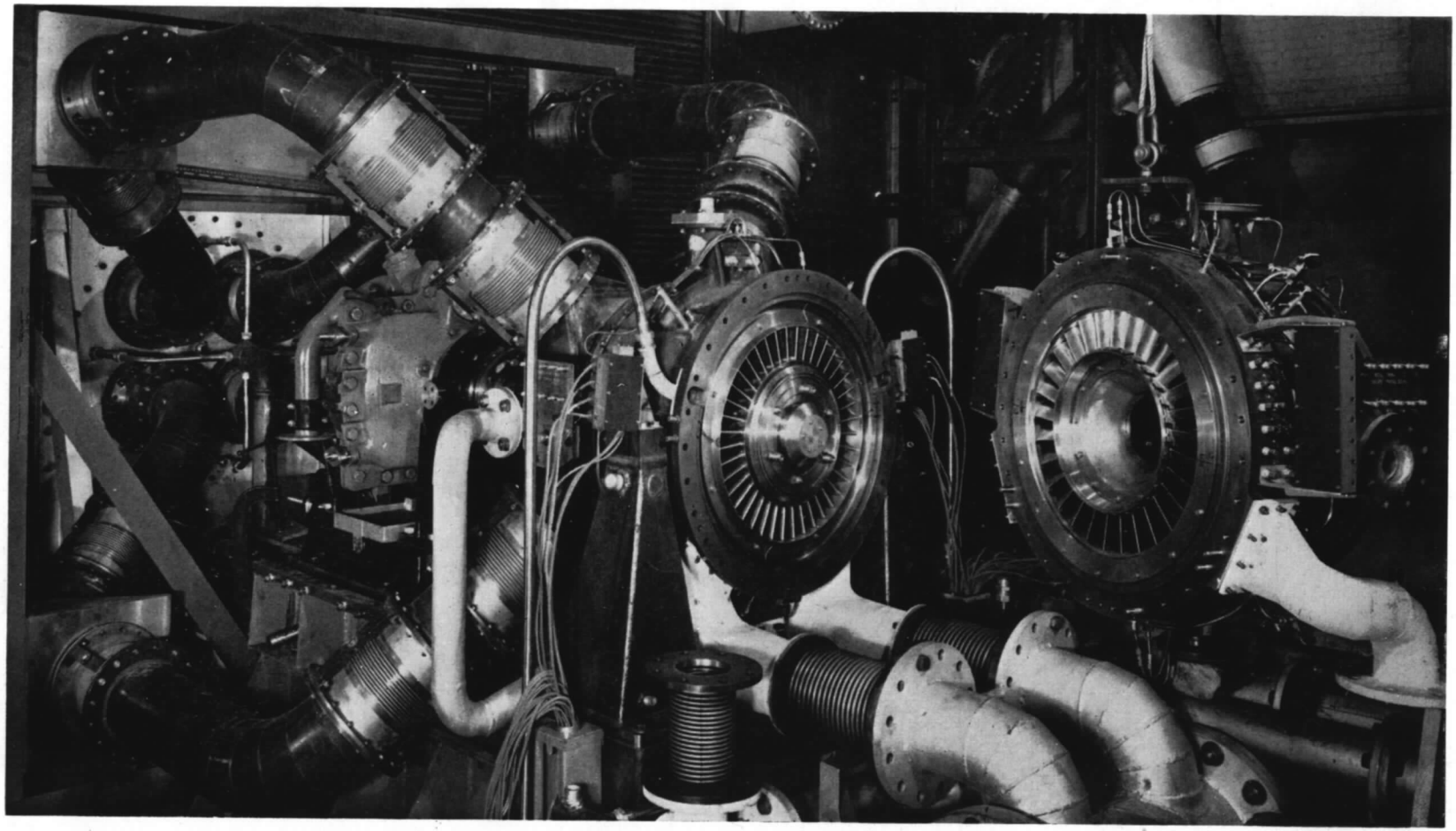

FIG. 1. No. 126 cooled turbine and test rig.

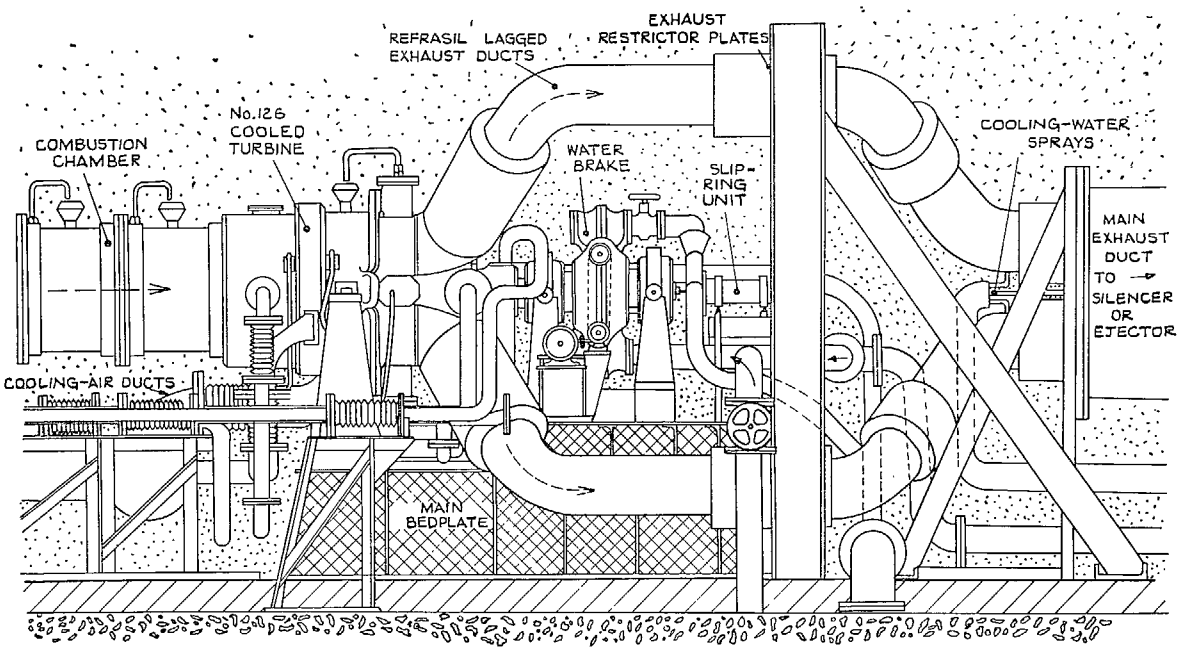

FIG. 2. No. 126 turbine test-rig layout.

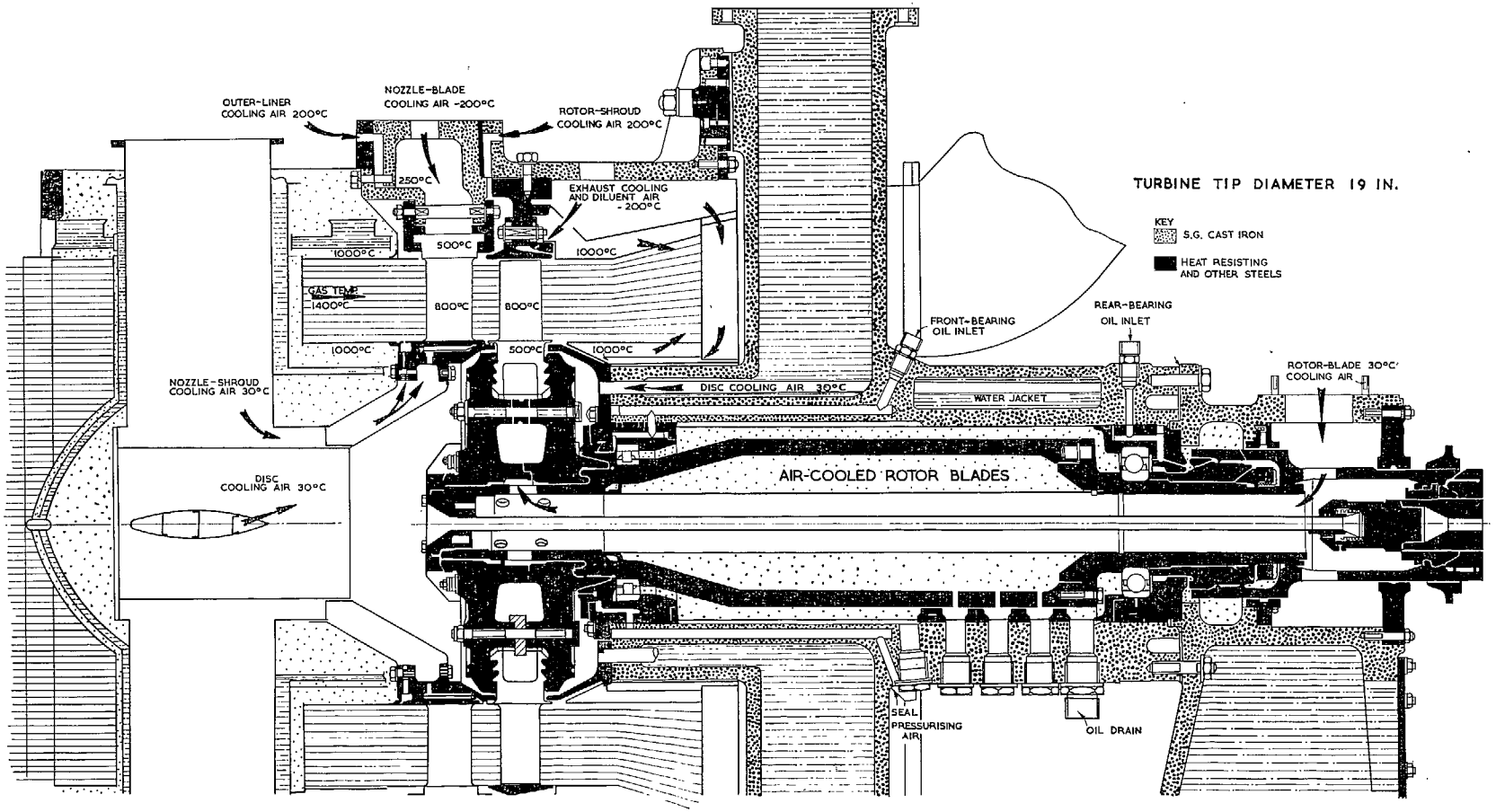

FIG. 3. No. 126 cooled turbine (sectional).

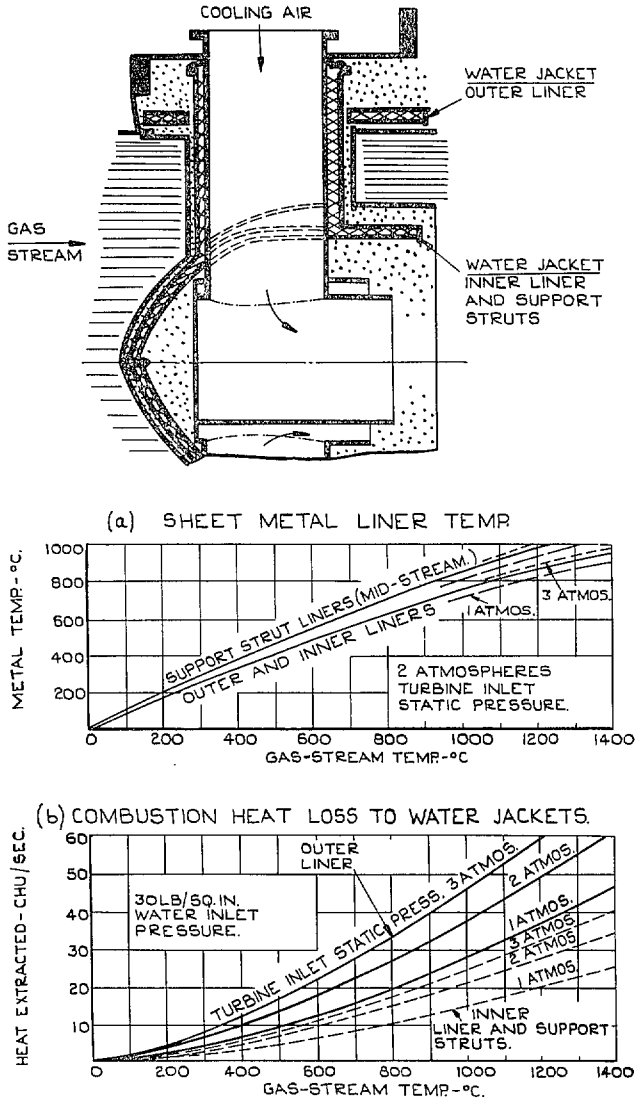

FIG. 4. Performance of turbine inlet assembly.

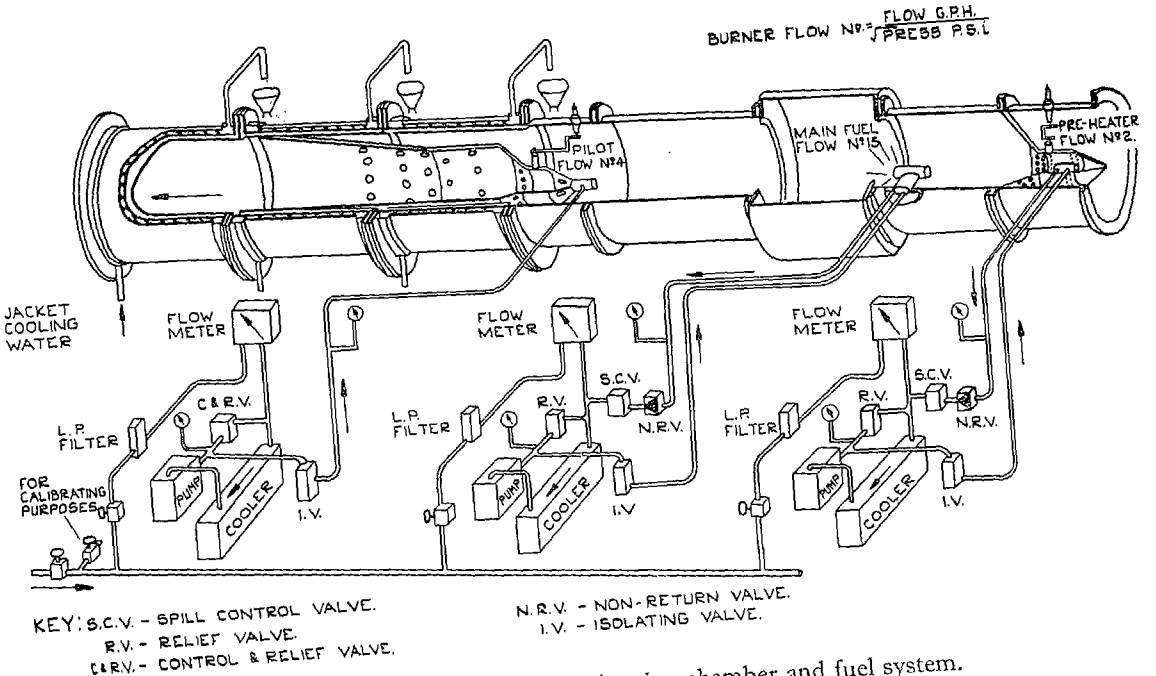

FIG. 5. High-temperature combustion chamber and fuel system.

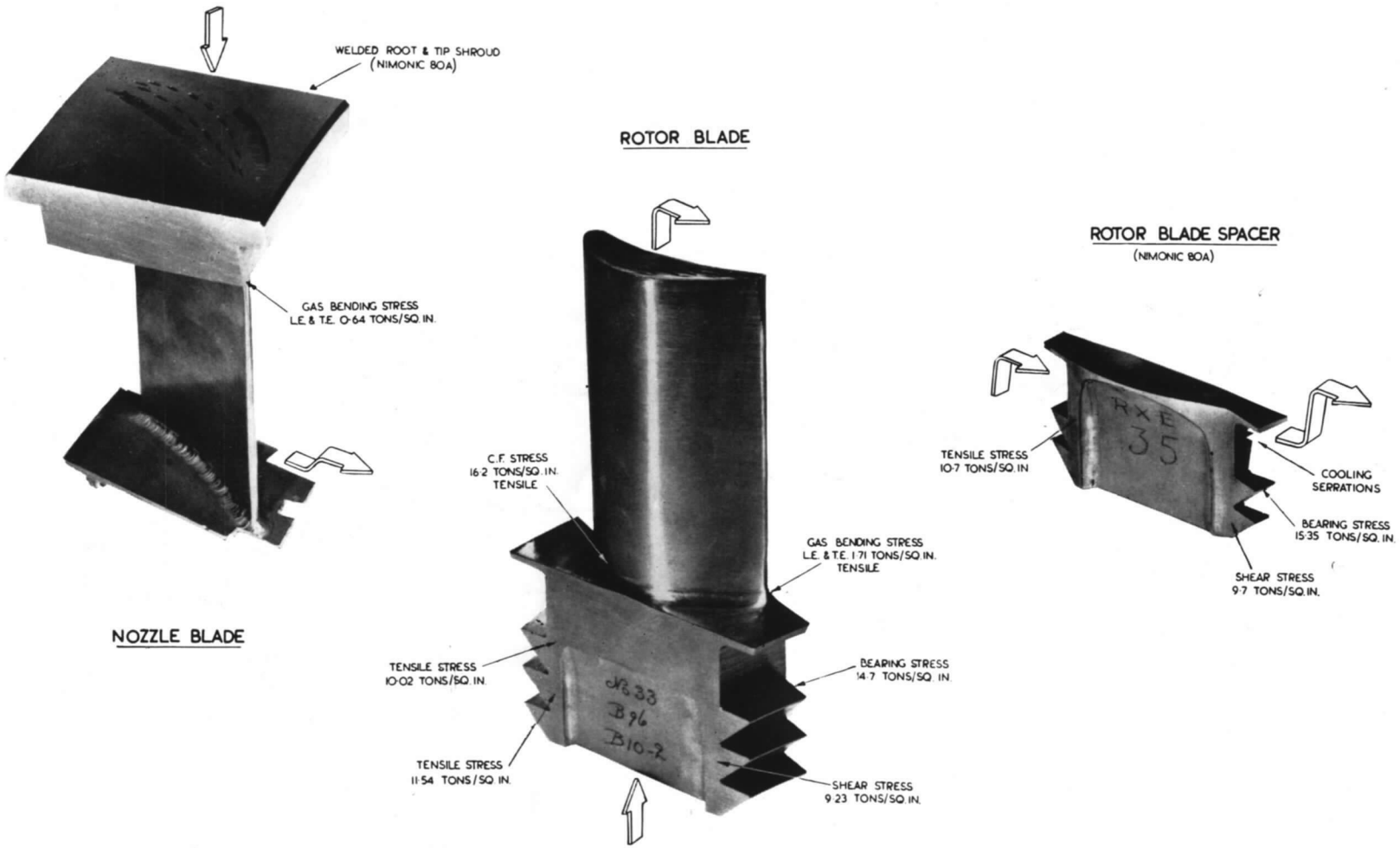

FIG. 6. Extruded Nimonic 90, air-cooled turbine blades (stresses at 13 300 rev/min).

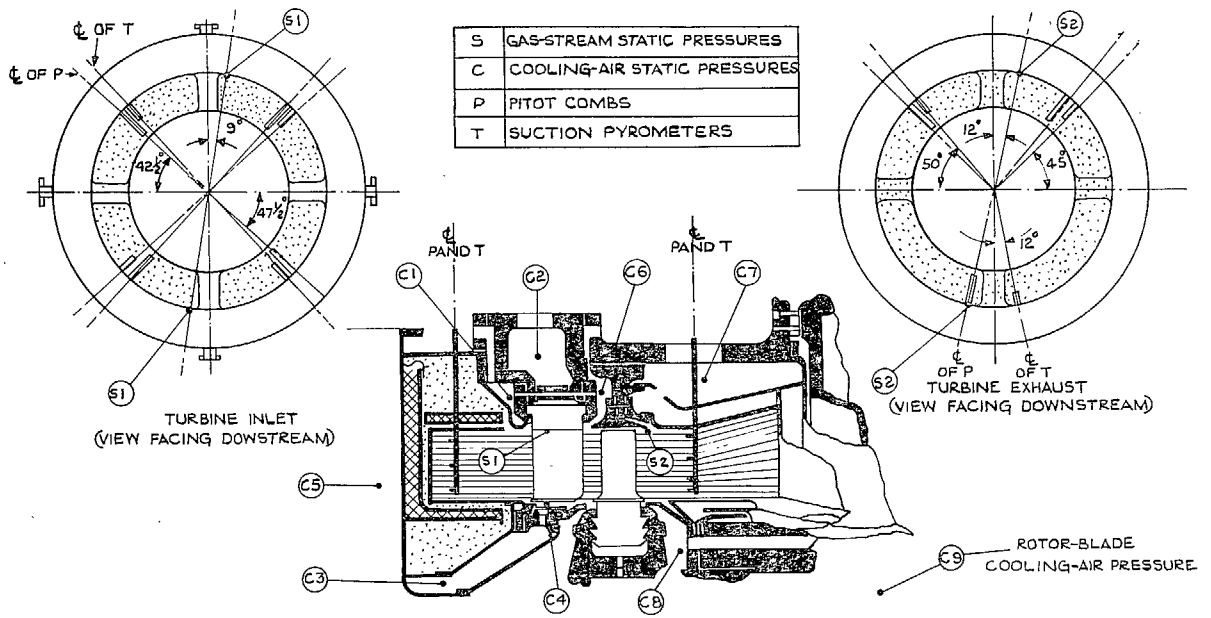

FIG. 7. Instrumentation in turbine annulus.

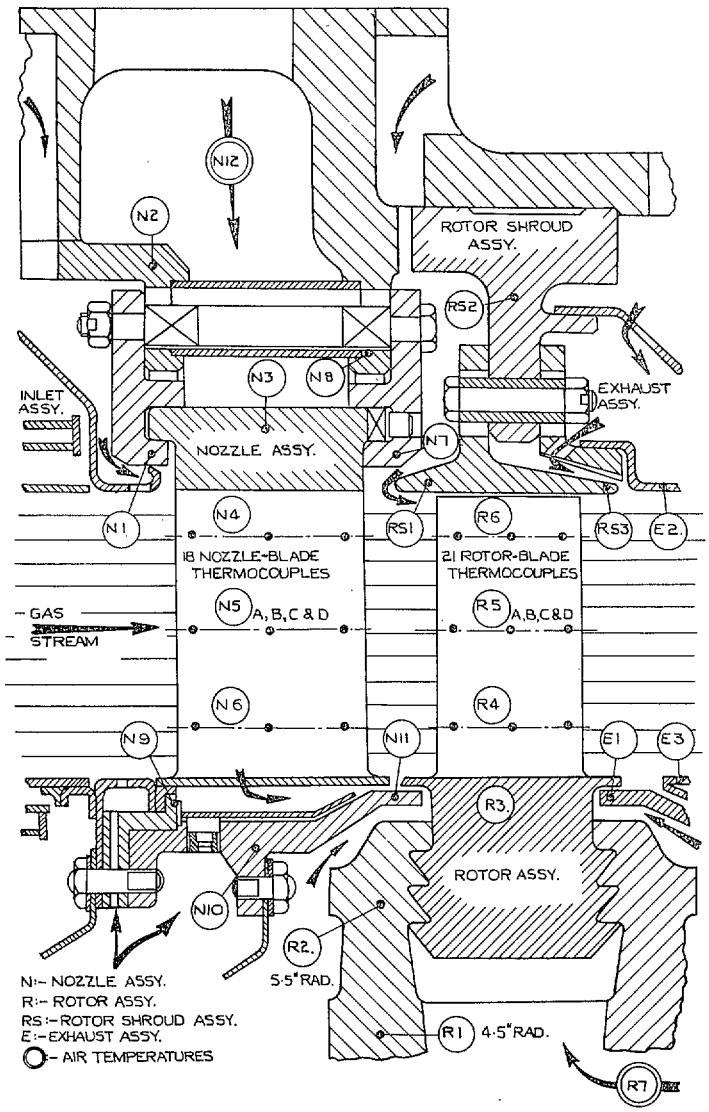

FIG. 8a. Thermocouples in turbine and blades.

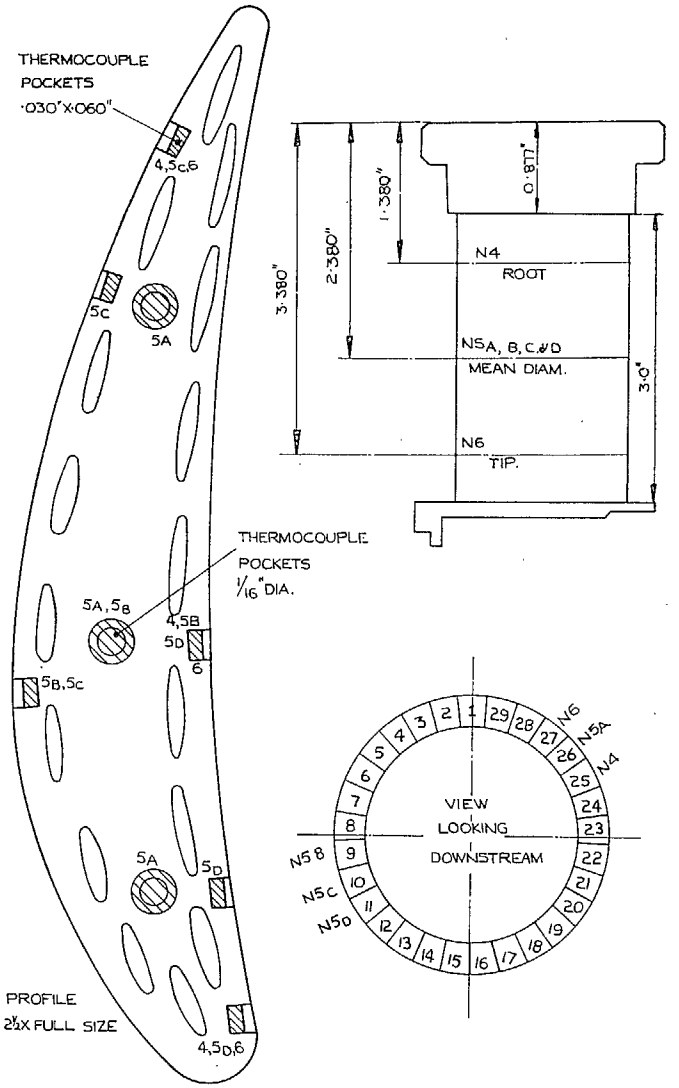

FIG. 8b. Thermocouples in extruded nozzle blades.

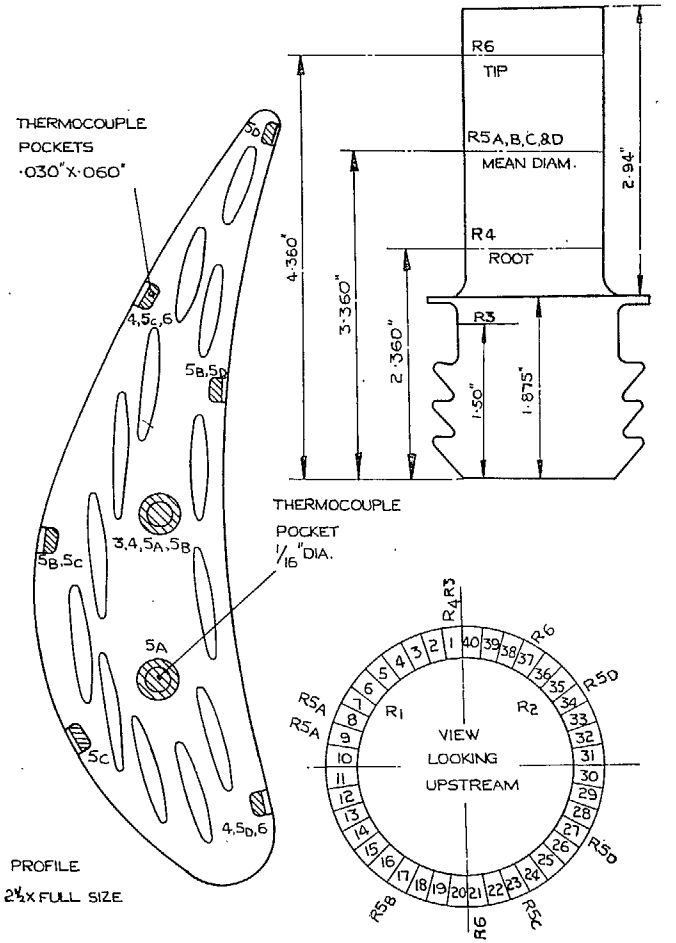

FIG. 8c. Thermocouples in extruded rotor blades.

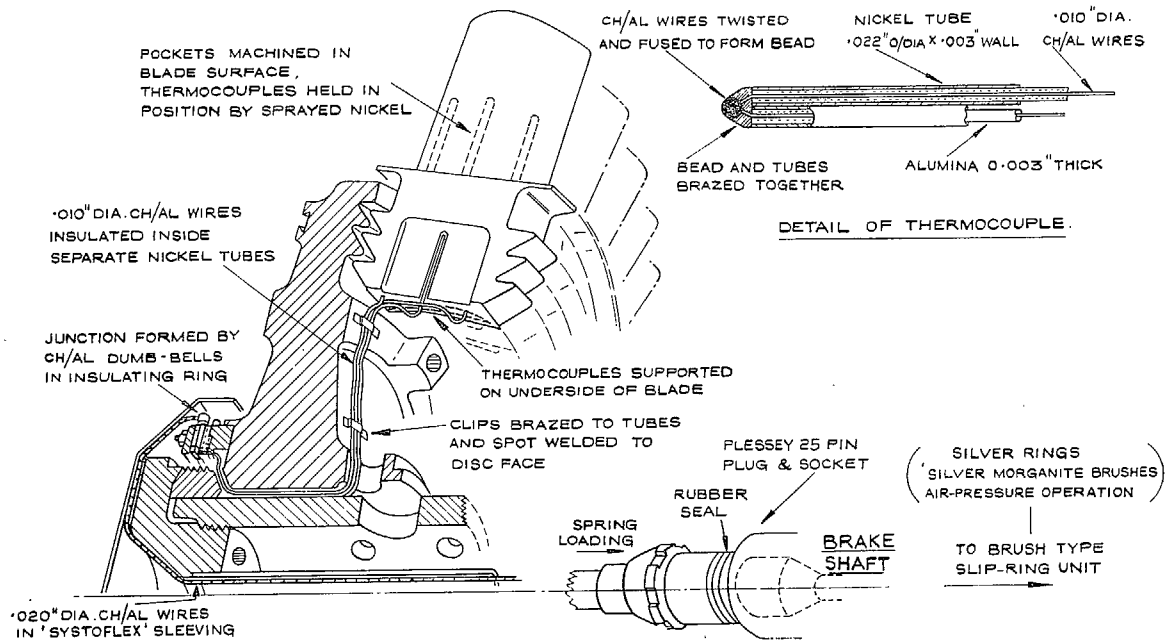

FIG. 9. Rotor-blade thermocouple system.

Part II.—The Behaviour of Extruded Air-Cooled Rotor Blades Subjected to Steady High Temperature and Rotational Speed

By J. F. BARNES, J. E. NORTHWOOD and D. E. FRAY

Summary.

Part II of this report describes the results of an endurance test at a gas inlet total temperature of 1500°K. Eighty hours of running were completed at a rotational speed of 12 000 rev/min with a rotor-blade cooling-air flow, equal to 1·8 per cent of the main gas flow, supplied to the rotor assembly at an inlet temperature of 310°K. During this period three blades failed in a manner similar to that predicted, and other blades exhibited spanwise cracks.

A method for estimating the redistribution of combined thermal and centrifugal stress in a non-uniformly cooled rotor blade due to creep effects is described and its predictions compared with observations.

LIST OF CONTENTS

Note on choice of scale of temperature

Since this report is concerned with blade behaviour and most of the physical and mechanical properties of blade materials are given at temperatures expressed in °Celsius (as opposed to °Kelvin), temperatures in this report have been expressed where possible in °C, with a concession for turbine gas and cooling-air inlet temperatures, which are more often expressed in °K when thermodynamic aspects of gas turbines are being discussed.

LIST OF APPENDICES

LIST OF TABLES

LIST OF ILLUSTRATIONS

---

1. *Introduction.*

In this Part more detailed information is given of the temperatures attained at various points in the extruded air-cooled rotor blades when the gas inlet total temperature was 1500°K. These temperatures were measured in the early stages of an endurance test at this gas inlet total temperature.

Eighty hours of interrupted running were completed at a speed of 12 000 rev/min with a rotor-blade cooling-air flow, equal to 1·8 per cent of the main gas flow, supplied to the rotor assembly at an inlet temperature of 310°K. These conditions were chosen in order to investigate the mechanical behaviour of the rotor blades when subjected to steady high temperature and rotational speed, and were deliberately made severe in order to obtain some form of blade failure or distortion within a period of about 100 hr.

It is known[1, 2, 3] that when a small quantity of cooling air is passed through rotor blades at a temperature which is considerably lower than the gas temperature, appreciable variations of temperature exist within the blades themselves, both in the spanwise and chordwise directions. The chordwise average of the blade temperatures measured in this investigation tends to rise from root to tip principally because the cooling-air temperature rises as it flows in this direction through the cooling passages. The non-uniform temperature distribution existing across any chordwise section occurs because it is relatively difficult to cool the leading and trailing edges as effectively as the mid-chord region where there is ample space for cooling passages. This chordwise non-uniformity of temperature, which, in these tests, has been accentuated by using small quantities of relatively cold cooling air, causes thermal stresses to be present, acting parallel to the spanwise axis and therefore modifying the uniform chordwise distribution of tensile stress produced by centrifugal effects. Because such thermal stresses are, to some extent, inevitable when air-cooled turbine blading is used, the main objective of the endurance test was to discover the effect of the resulting non-uniform stress distribution on blade life and to compare the actual behaviour of the blade material with predictions.

2. *Turbine Tests and Associated Stress Calculations.*

Details are given of the selected running conditions and of the measured blade temperatures at the chosen gas inlet total temperature (1500°K) with a blade-cooling air/main gas flow ratio of 1·8 per cent.

Methods of calculating blade stresses and the associated estimates of blade life are presented. At the end of this section the actual operating experience under steady conditions of high temperature and stress is described.

2.1. *General Description of Rotor Blades and Details of Running Conditions.*

The high-temperature experimental single-stage turbine has been described in detail in Part I of this report. Fig. 1 shows the chordwise section and an elevation of the cooled rotor blades used in the endurance tests. The blades were of untwisted constant section, and were extruded from Nimonic 90 cast stock. Thermocouples made from chromel and alumel wires of 0·010 in. diameter, insulated by alumina and sheathed in individual nickel tubes of approximately 0·020 in. diameter, were situated at the positions marked one to nine at the mean diameter. Similar thermocouples were also situated at some of the corresponding positions near the blade root and tip, particularly in the neighbourhoods of the leading and trailing edges.

The chosen operating conditions during the period of test running described in this report are given in Table 1.

It was known, from measurements of blade temperature at 1500°K gas inlet total temperature but at lower speeds, that the conditions given in Table 1 should produce combined centrifugal and thermal stresses severe enough to give a blade life of about 50 hours, using the rupture properties of Nimonic 90 given in Fig. 2a. These measurements of blade temperature had been obtained at a

gas Reynolds number (based on rotor blade chord and exit flow conditions) of 10^5. It was also known that if this Reynolds number was kept constant at 10^5 during an endurance test at 12 000 rev/min, the turbine would be running at a value of aerodynamic stage loading factor ($2K_p\Delta t/U_m^2$) equal to 1·6 and that the rotor blades would be operating at negative incidences over much of their height. It was therefore necessary to confirm that the blade temperature distributions would not be abnormal at negative incidences.

Measurements of blade temperature were made at the chosen endurance conditions and are shown on Fig. 3, together with those obtained at lower speeds (and therefore higher values of stage loading). The results are given in terms of blade relative temperature, defined[1] as $(T_{\text{blade}} - T_{cr})/(Tg_{\text{rel}} - T_{cr})$. Under endurance conditions the mean gas total temperature relative to the rotor blades (Tg_{rel}) was 1440°K, so that for a cooling air inlet temperature (T_{cr}) of 310°K, the ratio Tg_{rel}/T_{cr} was 4·64. At other speeds the values of Tg_{rel} and Tg_{rel}/T_{cr} were slightly different and corrections to the measured blade relative temperatures were applied to make all the results correspond to $Tg_{\text{rel}}/T_{cr} = 4{\cdot}64$. The required correction[1] did not exceed 0·03 in magnitude.

Fig. 3 serves to show that although the blade relative temperatures do vary slightly with the aerodynamic stage loading factor, the form of the blade temperature distribution at a stage loading of 1·6 is not markedly different from those obtained at loadings of 3·0 or more, where the incidence of the gas stream on to the rotor blades at the mean diameter is zero or slightly positive. (An estimation of the variation of incidence with stage loading is shown at the bottom part of Fig. 3. This figure has been split into three distinct parts to avoid confusion.)

The conclusion was therefore drawn from those blade temperature measurements that the calculated *thermal* stress distribution corresponding to the chosen high-speed and high-temperature conditions would not be unrepresentative of the thermal stress distribution obtained under the same gas mass-flow conditions and at a lower speed to give the design incidence.

An alternative method of obtaining the design incidence would have been to increase the gas mass flow and pressure ratio, keeping the speed constant at 12 000 rev/min. This would also have increased the Reynolds number to about $1{\cdot}5 \times 10^5$ and would have been expected to change the relative distribution of heat transfer from the gas to the blade surface, and hence to alter the chordwise temperature pattern. However, it was known that there is only a small difference between the shapes of the external heat-transfer distributions[4] at Reynolds numbers of 10^5 and $1{\cdot}5 \times 10^5$ and that this difference exists solely near the trailing edge. It seemed therefore reasonable to conclude that the changes in Reynolds number, and therefore in stage loading, would have a small effect on the general temperature and thermal stress pattern. Therefore the chosen operating conditions could be regarded as capable of producing a combined thermal and centrifugal stress distribution bearing some resemblance to that for zero incidence at the same speed.

It was also appreciated that the chosen mass flow imposed less arduous conditions upon the combustion chamber and other parts of the rig than those necessary to achieve zero incidence at 12 000 rev/min. (This was an important factor because some trouble was experienced with overheating of the water cooled walls of the combustion chamber during these tests. At a higher mass flow, the greater heat release from burning more fuel would have aggravated this overheating.)

2.2. *Rotor-Blade Temperature Distributions.*

On Fig. 4a, the spanwise variation of rotor-blade temperature is shown for the chosen endurance conditions. As a result of the rise in blade temperature from root to tip along the span of the blade,

the tensile stress to cause creep rupture after (say) 100 hr at any given spanwise position has its highest value at the root and falls toward the tip as shown in the Fig. 4b. Comparison of this stress, based on the estimated chordwise average temperature, with the distribution of centrifugal tensile stress at 12 000 rev/min indicates that the smallest difference exists at about 60 per cent of the span, which might therefore be expected to be the weakest position. The dashed line on the lower part of Fig. 4 shows the variation of stress to cause creep rupture after only 5 hr at the estimated leading-edge temperatures along the span of the blade. The implication here is that if induced compressive thermal stresses in the relatively hot leading-edge region did not reduce the resultant tensile stress to a value well below the average centrifugal tensile stress, at nearly all spanwise positions, the blade would have a very short life indeed.

Fig. 5a shows the measured variation of blade temperature across the chord at $l/L = 0{\cdot}6$. This temperature distribution was obtained wherever possible from the readings of thermocouples situated at the mean diameter ($l/L = 0{\cdot}5$), increased by approximately 20°C as shown in Fig. 4a. The average temperature was 810°C, with a peak value equal to 960°C at the leading edge. In those parts of the chord where measured temperatures were lacking, the distribution was made similar in shape to those shown in Fig. 14 of Ref. 1.

2.3. *Stress Calculations Assuming Perfectly Elastic Material.*

If it is assumed that the blade material behaves perfectly elastically, that plane chordwise sections remain plane† in the region of interest and that the blade itself is free to bend, a thermal stress distribution can be calculated by a simple method given in Appendix II. This method takes no account of shear stresses, direct stresses parallel to the chordwise plane or stress concentrations caused by the presence of cooling passages. It is completely valid if the blade section is slender and if temperature variations across its thickness are negligible at all chordwise positions. For thicker sections with substantial temperature variations across the thickness, however, the true stress distribution is of complex form such that at any point stresses and strains can exist in three mutually perpendicular directions and are inter-related by functions of Poisson's ratio. In the present blade the temperature variations across the thickness are much smaller than the chordwise variations and it has been assumed in consequence that stresses in all directions perpendicular to the spanwise axis are small in comparison with those parallel to it. This leads to an elimination of functions of Poisson's ratio and results in a great simplification of the equations for thermal stress and strain.

On Fig. 5b the thermal stresses calculated by this simplified method have been combined with the centrifugal tensile stress of $5{\cdot}9$ ton/in^2 existing at 12 000 rev/min at $l/L = 0{\cdot}6$. Values of Young's modulus and the linear coefficient of thermal expansion for Nimonic 90 were taken from the manufacturer's design data[5] and allowance was made for the variation of expansion coefficient with temperature. As in Ref. 3 gas bending stresses were disregarded. When operating at zero incidence, the maximum gas bending stress at $l/L = 0{\cdot}6$ is less than $0{\cdot}3$ ton/in^2. At negative incidence and reduced power output this stress will be even smaller and therefore insignificant. Vibratory stresses have also been disregarded because none of the measured resonant frequencies for the first and second flexural modes and the first torsional mode is close to possible excitation

† This assumption is completely accurate if the region of interest is at least one chord's length away from the tip of the blade (*see* N.A.C.A. Tech. Note 3778, Ref. 7). In other words it could be applied to calculate thermal stresses at the mid-span of a blade whose aspect ratio is 2 or more.

frequencies at 12 000 rev/min caused by either the nozzle blade wakes or the support spiders upstream of the nozzle blades. Excitation and resonance due to circumferential variations in gas temperature are even more unlikely.

In order to estimate the lives of different points in the blade, assuming that the estimated stresses did not change with time, recourse had to be made to stress/rupture data for extruded Nimonic 90, with and without holes. These data are given in Fig. 2 and show in Fig. 2b that the rupture properties of extruded Nimonic 90 without holes conform with the manufacturer's design data[5]. However, since it was known that the presence of holes packed with filler material during the extrusion process, could cause a weakening of the Nimonic 90, comparisons were also made between the estimated stresses and the data given in Fig. 2a for material extruded with holes. The N.G.T.E. tests were conducted on solid specimens of circular cross-section with a diameter of 0·232 in. and on specimens of 0·253 in. diameter, with five circular holes of diameter 0·044 in., symmetrically disposed with one hole along the central axis. The total cross-section area and perimeter of the holes have the same relationships to the total cross-section area of the specimen itself as those existing in the cooled blades. In general it will be noted that for a given stress and temperature the solid material lasts between two and three times as long as the material with holes.

This difference in life is further illustrated in Fig. 6. Here the elastic stresses on both the concave surface and the camber line at $l/L = 0{\cdot}6$ in the region $0{\cdot}2 < x/c < 0{\cdot}4$ have been compared with the stresses to cause creep rupture after 10, 30 and 100 hr. It appears that if the creep properties of the blade material correspond with the test data obtained from specimens with holes and if no change in stress distribution occurs due to creep, then cracks caused by creep (and hence failure) might be expected near the concave surface at about $x/c = 0{\cdot}22$ (where the stress is 14 ton/in^2 and the temperature is 830°C) after 10 to 20 hr. On the other hand, if the properties of the solid material apply, the corresponding 'life' might be 30 hr or more. These comparisons between the stress distribution calculated from experimental measurements of blade temperature and creep data may therefore be summarised at this stage by stating that the predicted blade life was about 20 hr after which creep cracks might have been expected at $l/L = 0{\cdot}6$, $x/c = 0{\cdot}2$ on the concave surface.

It must be emphasised that the creep life of Nimonic 90 at these temperatures is very sensitive to changes in stress and temperature: an increase of about 10°C in temperature or 10 per cent in stress is sufficient to halve the life to rupture. Therefore the agreement between a preliminary prediction of about 50 hr life (based on temperatures measured at lower speeds) and later estimates, from temperatures measured at 12 000 rev/min, of about 20 hr life is considered to be satisfactory.

2.4. *Redistribution of Stresses Due to Creep.*

It has been stated that the preceding comparisons had to be based upon the assumption that the calculated elastic stress distribution did not change with time. Examination of the different creep rates associated with the temperatures and calculated stresses at various points in the blade section indicates that comparatively rapid stress redistribution is probable, leading particularly to relief of local stresses near the leading edge where the material is hottest. This is borne out by the results of an attempt to calculate changes occurring in the stress distribution with time. The assumptions used and details of the method are given in Appendix III. For the purpose of showing the manner in which the stresses would change with time, the chordwise section of this rotor blade was divided into 24 elements. The stresses existing at the centroids of each of these elements were calculated using the method of Appendix II. The creep strains which would have occurred in bar specimens at the

values of stress and temperature corresponding to the conditions at the centroid of each element were estimated for a small time interval. The combined effect of these creep strains occurring in each element produced an area mean creep strain acting at the centroid of the chordwise section together with creep rotations about the principal axes. It was assumed that the plane section containing the centroids of all the elements before creep occurred remained plane at the end of the chosen time interval and in this way it was possible to compute the actual change of strain over the time interval in any element. The difference between this actual change of strain and the creep strain corresponding to the stress and temperature of that element gave the change of elastic strain and hence the change in stress.

Further stress changes were computed over later time intervals by using the assumption that the creep strain rate occurring at any point in the blade was equal to that measured in a test specimen under the same conditions of stress and temperature after a period of time equal to that which had elapsed from the commencement of stress redistribution. This is often termed 'time-hardening theory'.

Because creep-strain rates are very sensitive to changes in stress, particularly at high temperatures such as those near the leading edge of this blade, the calculations should either involve a series of iterations or be conducted over very small time intervals to avoid excessive stress changes. The second method was used in this investigation.

In Fig. 7 the changes occurring in the stresses at various points are given. The creep rates used for this calculation were based on Ref. 6 where the quoted lives to rupture at various stresses and temperatures correspond closely to the data given in Fig. 2b. It will be seen that relief of the compressive stresses near the leading edge is so rapid that they could not have existed for very long, if at all, in the tests on the rotor blades. During the gradual approach to the endurance conditions in which the speed and temperature were raised slowly, creep relief of compressive stresses would have been occurring in the blades. The only way by which the stresses calculated using Appendix II could probably exist, and then only for an infinitesimally short time, would have been some instantaneous loading process involving step changes in blade temperature. Since this is obviously impracticable, it must be concluded that the stress distributions given in Figs. 5 and 6 can only serve as a guide in assessing blade life. The value of such a stress distribution as a guide will be discussed later.

It may be argued that ultimately a stress distribution will be set up across the chord of the blade such that further changes in stress occur everywhere comparatively slowly. This would imply that the local creep rates corresponding to the stress and temperature distributions are nowhere very different from the actual strain rates caused by extension of the centroid and rotation about the two principal axes. It may also be argued that the final form of such a calculated stress distribution is not influenced very much by the initially calculated stress pattern but depends mainly on the blade material, the imposed temperatures and the rotational speed (*see* Section 4).

From Fig. 7 it may be concluded that such a stress distribution is approached after about 30 hr, when small tensile stresses exist near the leading edge and the tensile stresses at the coolest parts of the blade section have been reduced from the values calculated assuming that the blade material is perfectly elastic. Further changes in stress occur comparatively slowly. At this stage in the life of the blade the greatest creep strain exists not near the concave surface at $x/c = 0{\cdot}22$ but near the centroid where it is 8×10^{-4}. The worst combination of stress and temperature also exists, at this stage, in the neighbourhood of the centroid, having values of 16 ton/in^2 and 755°C respectively. These conditions correspond to a life of about 500 hr, using the data of Ref. 6, which, as previously

stated, correspond closely with Fig. 2b. The total creep strain at rupture of a Nimonic 90 bar specimen 16 ton/in^2 and 755°C is known[6] to be about 3 per cent. Bearing in mind that most of this observed strain occurs comparatively quickly over the later part[6] of the creep life, it may still be concluded that most of the redistribution of stress, as calculated by the method of Appendix III, has occurred comparatively quickly and with relatively little damage up to that point in terms of creep strain. At position 'B' on Fig. 7, for example, the stress after 1 hr appears to have fallen considerably from its original value giving an immediate improvement in predicted blade life. At 9 ton/in^2, 824°C, a life of perhaps 200 hr is indicated by the data of Fig. 2b, compared with about 20 hr at 16 ton/in^2.

If they ever existed, the *fully* redistributed stresses might be expected to confer a life of perhaps 1000 hr at the chosen endurance conditions using properties closely similar to those given in Fig. 2b. This corresponds closely with the value of life assessed on the simplest basis of all, namely the average blade temperature of 810°C and the centrifugal stress of 5·9 ton/in^2.

Available data from the creep tests on the extruded Nimonic 90 specimens with holes indicate that the observed rupture strains are not markedly different from those measured for solid material. This implies that creep rates in the material with holes are faster than those in the solid material, on average by a ratio between two and three to one. In other words the rate of redistribution might be expected to occur more quickly and failure near the centroid might occur after perhaps 300 hr. However, it will be shown later that the influence of holes on the life of extruded material does not manifest itself in such a simple manner.

The experimentally measured temperature distributions have therefore led to two extreme values of estimated blade life, corresponding to the two extreme assumptions of either (i) no redistribution of stress or (ii) a complete redistribution of stress in the very early part of the blade life. It now remains to compare these estimates with actual operating experience in the turbine and to discuss them in the light of evidence obtained from detailed metallographic and metallurgical examinations of the blade material.

2.5. *Actual Operating Experience under Conditions of Steady High Temperature and Speed.*

Whenever possible these tests were conducted for periods of between 3 and 5 hr at a time. After 16 hr of running, when most of the instrumented blades were replaced, no damage was visible on the external surfaces of any other blades. A further 9 hr of running were completed when one of the new blades failed. This blade had thermocouples embedded near the blade tip at the extreme leading and trailing edges. The failure occurred at approximately $l/L = 0{\cdot}6$, thereby tending to confirm that this was the weakest spanwise position, and is believed to have followed the following sequence. Creep failure commenced near the second cooling hole on the concave surface, i.e. near $x/c = 0{\cdot}2$, propagated across the thickness of the blade, put extra tension on the leading-edge region which then 'necked' and failed, and the blade finally broke at the trailing edge. Evidence in support of this sequence can be drawn from the colours of the oxide layers on the fractured surface. These were very dark grey between the camber line and the concave surface in the region $0{\cdot}2 < x/c < 0{\cdot}3$ and bright blue along the convex surface near the trailing edge. The darkest grey layer indicated that area of the blade section in which cracks existed for the longest period of time while the bright blue layer showed that part of the fracture which was subjected to the oxidising influence of the main gas stream for only a very short period of time, i.e. perhaps 15 sec between failure and shut down. A small area near the centroid of the blade section was also blue, indicating that the coolest part of the blade failed a short time before the trailing edge.

The cooling passages on this particular blade were closer to the concave surface than in most of the remaining blades. Since evidence presented later shows that Nimonic 90 is weak near the surface of any holes present during extrusion, it is quite conceivable that there was insufficient strength in the section of the blade between the cooling passage and the concave surface to withstand a combined stress of approximately 12 ton/in^2 at 830°C. The minimum thickness of material between the cooling passages and the concave surface of this blade was 0·015 in. at the position of the fracture rather than the nominal value of 0·040 in. Three other blades were removed for examination. One had been damaged by debris from the failed blade, another thermocoupled blade exhibited spanwise cracks between adjacent cooling passages at the tip and one, which had done 25 hr, appeared to be sound.

A second blade, also fitted with thermocouples, failed after 19 hr, when the total running time under endurance conditions was 35 hr. The proposed sequence for the failure of the first blade was confirmed by this second failure and a third, after 55 hr. Photographs of the second and third broken blades appear in Fig. 8. The third failure occurred in a replacement blade without thermocouples, put into the turbine when 25 hr endurance running had been completed. The total running time under endurance conditions when the third failure occurred was therefore 80 hr. At this stage the test was discontinued because no further reliable spare blades were available. There is very close similarity between the failures shown in Fig. 8. They differ slightly from the first failure in that the spanwise position of the fracture is nearer to the tip at the trailing edge than at the leading edge. Another difference is that no thermocouple crossed the plane of fracture of either of these blades.

Another blade put into the rotor to replace one of those removed at 25 hr exhibited a visible degree of bending along the span and many spanwise cracks running from root to tip. This distortion and cracking were first noticed when the second broken blade was removed. This distorted blade was removed at the same time. A sketch showing an exaggerated view of the bending is on Fig. 9, which also shows the positions of the spanwise cracks. This was the only blade to show any such distortion, and because the spanwise cracks were present to much greater extent than in any other blade it might be supposed that this blade developed some abnormal and unique defect during manufacture. It is therefore excluded from later comparisons between actual and predicted behaviour.

Many of the blades removed from the rotor were sectioned and examined. An account of the results of these examinations is given in the next section.

Operating experience has therefore tended to confirm that the region of the blade at $l/L = 0{\cdot}6$, $x/c = 0{\cdot}2$ was the weakest section. Further discussion of the wide range in observed blade lives is reserved for Section 4.

The cooling-air flows supplied to the other parts of the turbine stage were maintained at relatively high values throughout the tests in order to ensure reliable operation as far as possible. Some slight distortion of the unstressed liners in the inlet section and of the rotor shroud occurred. This last item appeared to have yielded plastically in compression at its inner diameter where it was hottest (800°C) and then to have distorted, with a general reduction in diameter, on cooling after each run.

3. *Metallurgical Investigations.*

It must be emphasised that the blades used in this turbine rotor were not all manufactured from the same batch of material or by exactly the same process. All the new thermocoupled blades put into the turbine after 16 hr operation were made from a second batch of material whose chemical

composition and creep properties, as determined by acceptance stress/rupture tests, were slightly different from those of the first batch. Details are given in Table 2 which indicate that the lives obtained from the stress/rupture tests were all longer than the values obtained from published data for Nimonic 90. The replacement batch of material appeared on this evidence to be better than the original.

The first air-cooled rotor blades were machined from billets which were heat treated after extrusion but prior to removal of the filler material from the cooling passages. Differential expansion (occurring during the heat-treatment process) between the filler material and the Nimonic 90 and residual strains produced by hot working are both known to cause enlarged grain growth, and hence some deficiency of the creep properties, in the material surrounding the cooling passages. The replacement blade billets were heat treated after leaching†. This tended to avoid the formation of enlarged grain growth, but caused oxide layers to be present instead. These oxide layers could also be expected to cause deficiencies in material properties. These points were borne in mind during the subsequent metallographic examination of blades removed from service and in conducting supplementary creep tests on specimens cut from used and unused blades.

As stated in Section 2.2, the extent of oxidation over the fractured surfaces tended to confirm the predicted position of the weakest part of each blade. These fractured surfaces were mainly intergranular and showed some evidence of shear near the trailing edge. There was also evidence of deformation and reduction of area, mainly in the first failure.

3.1. *Examination of Cracks within the Blades.*

No crack was found on the aerofoil surface of any of the other blades. However, the material between adjacent cooling holes in several blades contained cracks which ran in a spanwise direction. Some of these cracks were visible after cleaning and polishing the tip section of a blade and, more rarely, they were also visible at the underside of the root section, indicating that cracks were present along the length of the blade and might well have been present in the extrusion before testing commenced. This last supposition is supported by the presence of small cracks in two of the unused blades which were examined. Other cracks were only revealed when blades were sectioned, as for example, when two apparently sound blades, removed after 16 and 25 hr respectively, were examined. These blades had spanwise cracks existing between adjacent cooling passages in the neighbourhood of the leading edge at approximately mid-span. Oxide layers were detected between the opposite faces of these cracks indicating that the cracks had existed within the blades for some considerable time. The cracks were intergranular and had opened, indicating that tensile stresses had existed across the material between the cooling passages. A typical example is shown in Fig. 10a. It is of interest to note than spanwise cracks had not propagated across the material between adjacent cooling passages in the first fractured blade which was sectioned and examined extensively. One almost complete crack was found between leading-edge holes on the third fractured blade. Small fissures and cracks were observed emanating from the cooling-passage walls of various blades, including the first fractured blade. These are described further in the next section.

In both the first and third fractured blades, creep-type intergranular cracks were very marked near the fracture. No crack was found at distances greater than about 0·5 in. from the fracture surfaces and in both blades the concentration of cracks was greatest near the leading edge. Farther away from the fracture, cracking gave way to fine intergranular cavitation.

† This process was also used for the creep-test specimens used to obtain Fig. 2a.

Sections of the bent blade near the leading-edge cooling passages also revealed well-defined creep cracks running transverse to the spanwise axis of the blade. None of these had propagated to the outside surface, suggesting that failure had originated around the cooling passages. A photomicrograph of this cracking appears as Fig. 10b.

3.2. *Examination of Material Taken from the Neighbourhood of the Cooling-Passage Surfaces.*

Complete chordwise sections of the blade were taken at various spanwise positions. Several longitudinal sections were also taken in the neighbourhood of $l/L = 0{\cdot}6$. As stated in Section 3, several small cracks and fissures were observed emanating from the cooling-passage walls of various blades. In sections of the replacement blades these fissures contained oxide and had developed from the intergranular oxide layer along the walls of the holes. This layer was usually 0·001 to 0·0015 in. thick over the walls of the elliptical passages but increased to 0·003 in. at the ends of the major axes. In the original batch of material no such oxidised layer was found but the surfaces of the holes were rough as a result of the leaching process used during manufacture. At the ends of the major axes the leaching solution had attacked the surrounding material, producing intergranular fissures.

Both the oxidised fissures and the results of leaching attack on the ends of the major axes of the cooling passages were considered to be potential sources of weakness. The former sometimes penetrated to much greater depths (0·007 in.) and were regarded as the more serious of the two types. However, both could cause concentrations of any stresses acting parallel to the axis Oy in Fig. 7.

Severe grain growth in the region of the cooling holes was most marked in the original batch of blades and resulted in a coarse-grained envelope 0·020 in. to 0·030 in. deep round most of the cooling passages (Fig. 11a), so that the thin web of material between adjacent passages and thin sections between passages and the blade surface were often completely coarse grained. On the replacement batch coarsening was limited to incomplete narrow bands 0·010 in. to 0·015 in. deep (Fig. 11b) which nevertheless still resulted in the web between some passages being completely coarse grained.

An explanation for the differences in oxide layers and grain coarsening around the cooling passages of the original and replacement blades has already been given. Further grain growth around the cooling passages could occur after extrusion due to the presence of residual strains. As little as 1 per cent plastic strain can induce such grain growth and this is the probable explanation for the grain growth observed in the replacement batch of material.

The results of several creep tests conducted on sub-miniature specimens taken from various parts of the unused blades indicate that the material in the roots and aerofoil sections away from the cooling passages was not sub-standard when compared with tests on specimens of the same size taken from forged stock. However, tests on several strip test pieces, taken from between cooling passages as shown in Fig. 11c, reveal a marked weakening of the material in these regions, particularly when it was coarse grained. Tests conducted on 0·020 in. × 0·120 in. rectangular test pieces at 11·5 ton/in², 830°C, gave lives of 34 hr† in forged material, 19 hr on fine-grained extruded material and 9 hr on coarse-grained extruded material. This suggests that blades manufactured from the original batch of material might be expected to have shorter creep-rupture lives than those of the replacement batch. It must be remembered, however, that the effect of oxidation at the surface

† It must be remembered that the size of test specimen influences creep life to rupture. Under the same conditions a forged 0·1 in² round test specimen would be expected to fail after 150 hr.

of the cooling passages on creep-rupture life would not be revealed by these tests because it was necessary to machine the test pieces. Nevertheless a minimum of material was removed and in some instances traces of the original surface were still visible. Failures were not found to emanate from these traces.

All the evidence so far seemed to indicate that while all the blades which had broken or bent had been made from the replacement batch of material, this did not appear to be in any way inferior to the original batch. It was thought therefore that some degree of over-ageing had occurred in the original blades, which had completed many hours operation at lower temperatures, and that this over-ageing had had a beneficial effect during the endurance test. Two creep test-pieces from a reference material were therefore heated for 200 hr at 700°C prior to stress/rupture testing at 12 ton/in^2 and 830°C. The results were compared with those obtained on two corresponding test pieces subjected to standard[5] heat treatment. No significant difference in life was detected.

3.3. *Structural and Hardness Changes Observed in Blade Sections.*

At temperatures between 920°C and 1020°C, depending on the exact composition of the Nimonic 90, a structural change occurs which can be detected by metallographic methods. This structural change is caused when the γ' phase precipitate† returns into solution and is accompanied by a coarsening of carbide and γ' phases at the grain boundaries; the extent of the coarsening may be modified by the presence of stress. Subject to this last proviso, metallographic observations can be used to estimate the approximate temperature attained by a given section of a blade, provided that the time of heating is also known.

Sections were taken from blade roots and heat treated over a range of temperatures for approximately the same time as a given blade had been under test. Microstructures of these root sections were then compared with structures obtained on the blade itself. At the same time a change in hardness, which was also time and temperature dependent, occurred with the structural changes in the material and was measured in order to obtain confirmation of the temperatures deduced by metallographic examination.

Several chordwise microsections of unbroken blades from the original batch showed the boundary of a 960°C/980°C isothermal across the blade section, as in Fig. 12, for $l/L = 0{\cdot}75$. A similar isothermal could be drawn at 940°C/960°C for the replacement batch. Precise correlation between structural changes and temperature was not possible away from these temperature ranges. Temperatures estimated from Vickers hardness tests on the material are also shown on Fig. 12. Some discrepancy exists between the temperatures derived by the different methods. This may be caused to some extent by variations in local composition known to exist in Nimonic alloys. These cause the resolution of the γ' phase to occur non-uniformly so that the estimation of positions representing a definite degree of resolution becomes more difficult and the scatter in hardness measurements increases.

Other sections of unbroken blades at $l/L = 0{\cdot}5$ and $l/L = 0{\cdot}375$ were also examined and their structural conditions appeared to agree fairly well with temperatures obtained on thermocoupled blades. Wherever possible, corresponding sections from failed blades and from the bent blade were examined in an attempt to ascertain whether overheating of these blades had contributed to their failure. A section of the bent blade at $l/L = 0{\cdot}71$ gave low hardness values over a considerable

† The γ' phase is Ni_3 (AlTi).

area of the blade together with a structure in which the γ' phase was predominantly in solution. Both these observations suggest that the blade had operated at an abnormally high temperature.

Sections at $l/L = 0{\cdot}375$ on the first and third fractured blades were also examined. On the first fractured blade the γ' phase solubility line could be detected, while on the reference blade, from the original batch of material, no definite indication of resolution of the γ' phase could be found. The different temperature level of this line in the two batches of material would partly account for this. Hardness measurements however indicated that the first fractured blade had been some 50°C hotter in the region between the leading-edge cooling passages. Both hardness and microscopic examination on a similar section of the third fractured blade failed to reveal any indication of overheating. Limitations inherent in the hardness measurements and in the observation of structural changes did not allow any conclusion to be formed as to whether there had been any overheating of the first fractured blade on or near its concave surface at $l/L = 0{\cdot}375$. This was because the temperatures were too low for the observation of any phase change and the wall of material between the concave surface and the cooling passages was too thin to permit satisfactory hardness measurements. In addition, the presence of cracks, and other structural features indicating strain in the material, prevented comparisons on chordwise sections nearer to the fractures on these two blades.

As a check on the initial uniformity of hardness of material in these blades, similar measurements were made on an unused blade and showed no systematic change in hardness near the leading edge.

4. *Discussion.*

As stated in the Introduction, the choice of operating conditions in the endurance test was governed by the requirement that if possible some form of blade failure or distortion should occur within about 100 hr. Allowance had to be made for possible stress redistribution which meant that the expected blade life, based upon calculated elastic stresses and measured temperatures, would have to be somewhat less than 100 hr. At the same time it was desirable to avoid excessively high temperatures in the blades and to avoid the associated occurrence of phase changes and ageing processes within the material to extents which would not normally be encountered in engine blades running at lower temperatures over much longer periods of time.

The measured blade temperature distribution and the speed of 12 000 rev/min, giving a predicted life of 20 hr (based on elastic stresses), was considered to be a reasonable compromise at the commencement of the endurance test. As events unfolded, with blades breaking at 9 hr and 19 hr and evidence of some phase change occurring in a small region near the leading edge, it might have been argued that the operating conditions were too severe and unrealistic. Later experience, with another failure after 55 hr and some blades lasting over 80 hr, tends to disprove this, and the tests have been of some value in confirming the simple method of predicting the weakest spanwise position of the air-cooled extruded rotor blades, because all three failures occurred at $l/L = 0{\cdot}6$.

Furthermore, the very simplified method of calculating thermal stresses, given in Appendix II, resulted in the prediction that $x/c = 0{\cdot}22$ on the concave surface was the weakest part of the chordwise section at $l/L = 0{\cdot}6$ and that creep cracking should be expected to occur first at or near this point. The tests were again of value because this prediction was to some extent confirmed by examination of all three failed blades. Creep cracking was found near the leading edges when two of these blades were sectioned. The appearance of the oxide layers on the fractures themselves also indicated that cracking had occurred first near $x/c = 0{\cdot}2$ between the concave surface and the camber line. There are, however, modifying features which must be taken into account.

The first of these is that more complicated methods[7] of estimating the stress distribution existing in the blade show that the direct thermal stresses acting parallel to the span increase from zero at the blade tip and only approach the values calculated by the simplified method at a distance from the tip approximately equal to the blade chord. In other words the assumption that 'plane sections remain plane' is reasonable between the root and the mid-span regions of this blade. At $l/L = 0{\cdot}6$, the method of Ref. 7 indicates that the maximum tensile thermal stress would be calculated to be about 85 per cent of the corresponding value obtained by the simplified method. The agreement between the stresses calculated for $l/L = 0{\cdot}6$ at other chordwise positions appears to be even better. As a result of this comparison between methods of calculating stresses, the direct spanwise stresses as shown on Fig. 5b lead to a pessimistic prediction of blade life (on the assumption that the blade material remains perfectly elastic, with no stress redistribution occurring).

This introduces the second modifying feature, namely the redistribution of stresses within the blade due to creep.

In Section 2.1 it was argued that some relief of stress must occur, particularly at the very hot leading edge. A possible change of stress distribution was described in Fig. 7 which showed that after 30 hr the blade might have reached a condition where subsequent stress changes occurred comparatively slowly. It must be emphasised that the method derived for this calculation also makes use of the simplifying assumption that 'plane chordwise sections remain plane' in the region of interest, during the stress redistribution process. There is little experimental evidence in support of this. All that can be said at this stage is that the stress-relief method predicts blade distortions which have actually been observed in practice, in an earlier[3] investigation. It will be recalled that under the influence of centrifugal, thermal, and gas bending stresses, the rotor blades used in Ref. 3 distorted in a manner very similar to that shown on Fig. 9. However, a laboratory test on a stationary blade subjected only to thermal stresses caused distortion in the opposite direction. Calculations on simplified arrays representing such a blade with and without centrifugal stress have been performed and the calculated modes of distortion agreed with the experimental observations. The distortion of the bent blade shown on Fig. 9 cannot be regarded as a confirmation of the stress-redistribution calculation because of the abnormally severe spanwise cracking and the evidence of overheating.

Calculations performed on similar simplified arrays also showed that substantially the same fully relieved stress distribution was approached, whatever the values of the initially calculated stresses, provided that these last were not completely unrealistic and satisfied the loading conditions imposed on the blade. The time taken to approach such a fully relieved distribution obviously varied with the initially assumed stresses, but this exercise did show that the fully relieved stress distribution depended mainly upon the material properties, the imposed temperatures and the rotational speed. This is worth emphasising because the effects of plastic deformation during the loading process have not been included in the calculation of the initial stress distribution. It is perhaps reasonable to suppose that such plastic deformation would cause changes in the initially calculated stresses similar to those produced by creep in the very early stages of the stress-redistribution calculation. If this supposition is correct, plastic relief would clearly allow blade lives in this investigation to be much longer than 20 hr, although less than the 1000 hr corresponding to the fully relieved stress distribution.

Another assumption which had to be made was that compressive creep-strain rates were equal in magnitude but opposite in sign to those measured for corresponding tensile stresses. There is little evidence to confirm or disprove this for Nimonic 90.

The process of stress redistribution, involving as it does the reduction of the stresses at the most severely loaded part of the blade, brings with it an improvement in blade life as compared with predictions based on 'elastic' stress distributions. Although four blades exhibited some form of creep failure, after times which agree in magnitude with the simple predictions given on Fig. 6, the evidence that stress redistribution occurred arises from the fact that many of the original blades lasted for over 80 hr, and some of the replacement batch lasted for over 60 hr. It must also be remembered that the first fractured blade and the bent blade which were both removed after 10 hr operation, appear to have been overheated and also that deficiencies in material properties have been detected in the vicinity of cooling passages.

These deficiencies represent the third and last modifying feature. It would clearly be very difficult, if not completely impossible to take account of this when estimating the life of a blade. The influence of an oxidised layer on the surfaces of passages in extruded creep-test specimens subjected as nearly as possible to uniform direct stress has been shown to reduce creep-rupture lives to between one half and one third of those measured on solid specimens. The cross-section area and perimeter of these passages have the same relationships to the total cross-section area of the test specimen as those existing within the cooled rotor blades. It is quite possible however that local concentrations of enlarged grain growth and other sources of weakness were present to quite different extents in the test specimens and the blades. Moreover the latter were subjected to a non-uniform stress and temperature distribution where the most critical combination of stress and temperature was between the walls of a cooling passage and the blade external surface. Any deficiency of material properties in the vicinity of that cooling passage and external surface would then be expected to have the most adverse effect and to manifest itself as a premature blade failure, especially if the thickness of material between the outer surface and the cooling passage was less than the nominal value. This would explain the failure of the first blade after a comparatively short time, even if some stress redistribution had occurred.

It is also quite plausible that sources of weakness such as fissures and enlarged grain size contributed to the failures of the other two blades, and that they were not present to the same extent as in the first failed blade.

The absence of any failure in the blades of the original batch, except for spanwise cracks, is significant and tends to support the statement in Section 3.2 that fissures emanating from the oxidised surfaces of cooling passages in the replacement material are potentially a greater source of weakness than smaller fissures caused by leaching attack in the original material

So far no mention has been made of direct stresses acting parallel to the chordwise plane. Ref. 7 shows that they are likely to be small compared with the stresses acting parallel to the span, especially at distances greater than one chord length from the free end. However, the fissures emanating from the surfaces of the cooling passages could cause considerable local stress concentrations and thereby accelerate blade failure.

Some metallurgical evidence has been put forward in Section 3.3 indicating that part of the leading-edge region of the first failed blade was overheated, particularly between the three cooling passages. Calculations indicate that such local overheating, of about 50°C, could occur in this region if the total cooling flow to the blade was reduced from 1·8 per cent to 1·73 per cent of the main gas flow, and all this reduction was concentrated in these leading-edge passages (so that their individual flows were some three quarters of the average flow through the same passages in other blades). The reduction in overall flow would be within the limits of scatter obtained in preliminary

pressure-drop calibrations and examination of the remaining portion of this blade shows that the entry sections of the leading-edge holes were in fact slightly restricted. Moreover it is not possible to state whether or not overheating occurred at the most severely loaded part of the blade, on the concave surface, where it would have the most serious effect on creep behaviour and on life to rupture.

The apparent general overheating of the bent blade is more surprising; no thermocouple was installed in this blade and examination of the pressure-drop calibration would not suggest that this blade had been starved of cooling air to such an extent that all of its chordwise section was at a temperature over 920°C at $l/L = 0{\cdot}71$. However, it must be conceded from the behaviour of this blade in the turbine that parts of it, at least, had been overheated, and the only other known contributory feature is the presence of spanwise cracks. Examination of Figs. 9 and 10a shows that such cracks could impede the flow of heat from the outside surface to the cooling passages. This would not, however, be expected to cause general overheating.

It must be admitted that the general picture emerging from this discussion on the probable life of air-cooled turbine rotor blades is complicated. It may be summarised by stating that 'first order' methods exist for predicting the weakest part of a blade and for allowing stress redistribution to be calculated from the creep properties of the material. If the blade approaches a state where stress redistribution is almost complete, it can have a very long life compared with estimates based on the assumption that the original 'elastic' stress distribution does not change with time. The degree of redistribution which occurs, before failure supervenes, appears to be limited in the present extruded blades. Failure seems to have been governed very substantially by other factors such as local deficiencies in material properties, caused by fissures or enlarged grain structure near the surfaces of cooling passages.

5. *Conclusions.*

(i) Rotor-blade temperatures have been measured at gas inlet total temperatures up to 1500°K at various turbine speeds for a Reynolds number, based upon blade chord, of 10^5. The temperatures were generally insensitive to gas incidence.

(ii) The turbine was operated satisfactorily for a total period of 100 hr with a gas inlet total temperature of 1500°K. Eighty hours were completed at a speed of 12 000 rev/min with cooling air, equal to 1·8 per cent of the main gas flow, fed to the rotor blades at an inlet temperature of 310°K.

(iii) The predicted weakest spanwise position of these rotor blades, obtained by comparing centrifugal stresses and the spanwise variation of blade temperature, was at $l/L = 0{\cdot}6$. This was confirmed by the failure of three blades, all at $l/L = 0{\cdot}6$.

(iv) The estimated thermal and centrifugal stress distribution at $l/L = 0{\cdot}6$ (calculated assuming that the blade is free to bend, behaves perfectly elastically and that plane chordwise sections before the superposition of the temperature distribution remain plane afterwards) indicated a blade life of about 20 hr with failure starting at $x/c = 0{\cdot}22$ on the concave surface. This prediction of the failure position has been confirmed experimentally. The three blades which failed did so after 9, 19 and 55 hr respectively.

(v) If complete stress redistribution could occur, the blade life would be expected to be approximately 1000 hr. The actual degree of redistribution, before failure supervenes,

appears to be limited in the present blades. Failure seems to have been governed primarily by deficiencies in the strength of the material of the blade in the neighbourhood of cooling passages.

(vi) Metallurgical investigations indicate that extruded Nimonic 90 material, taken from parts of the blade away from the cooling passages, compares favourably in its creep properties with forged material. Enlarged grain growth and more particularly fissures emanating from the walls of cooling passages are potential sources of weakness. These weaknesses probably caused the lives of creep-test specimens extruded with holes to be between one half and one third of the lives measured with solid specimens under the same conditions of stress and temperature. A local concentration of such weak material, especially in an area known to contain the most severely loaded part of a blade, would have the most adverse effect on blade life, manifesting itself as a premature blade failure. Under such conditions the life of a blade might be expected to be very much less than a third of the predicted value of 1000 hr, based upon creep-rupture data for solid material and upon a stress distribution which includes the effect of creep relief.

REFERENCES

No.	*Author(s)*	*Title, etc.*
1	D. E. Fray and J. F. Barnes ..	An experimental high temperature turbine (No. 126). Part I.—The cooling performance of a set of extruded air-cooled turbine blades. A.R.C. R. & M. 3405. December, 1962.
2	D. E. Fray and N. E. Waldren ..	Investigations on an experimental air-cooled turbine—Part III. A.R.C. R. & M. 3144. January, 1958.
3	N. E. Waldren and C. J. Hart ..	Investigations on an experimental air-cooled turbine—Part IV. A.R.C. R. & M. 3144. January, 1958.
4	D. G. Ainley	Internal air cooling for turbine blades. A general design survey. A.R.C. R. & M. 3013. March, 1955.
5	Henry Wiggin and Co. Ltd. ..	The Nimonic series of high temperature alloys. Publication No. 2358, 8th edition. August, 1961.
6	K. F. A. Walles	A quantitative presentation of the creep of Nimonic alloys. N.G.T.E. Note NT. 386. A.R.C. 20 935. March, 1959.
7	A. Mendelson and M. Hirschberg	Analysis of elastic thermal stresses in a thin plate with spanwise and chordwise variations of temperature and thickness. N.A.C.A. Tech. Note 3778. November, 1956.

APPENDIX I

Notation

A	Element of cross-section area when in a chordwise section of the blade
C	Creep strain
E	Young's modulus
K_p	Gas specific heat at constant temperature
T	Temperature
U_m	Mean blade speed
l, m	Constants in equation (3) Appendix III, defined by equations (6) and (7) respectively
p, q	Constants in equation (4) Appendix II, defined by equations (10) and (11) respectively
x, y	Coordinates defined on Figs. 1 and 7
α	Coefficient of thermal expansion
ϵ	Strain
σ	Direct stress
ϕ	Rotor-blade cooling-air mass flow/main gas mass flow

Subscripts

cr	Refers to cooling-air conditions at entry to the blade root
g_{rel}	Refers to gas conditions relative to the rotor blades
j	Refers to any element in a blade section which has been divided into n elements
$\mathbf{0}$	Refers to conditions at the centroid of a blade section

APPENDIX II

Thermal Stresses with Young's Modulus and the Linear Coefficient of Thermal Expansion Variable with Temperature

Let ϵ_j be the actual strain at a point j when heated through a temperature rise T_j.
The thermal stress at this point is given by the equation

$$\sigma_j = E_j(\epsilon_j - \alpha_j T_j).$$

If we consider an unloaded specimen, subjected only to thermal stress, the resultant moment produced by the stresses about mutually perpendicular axes in the plane of cross-section must be zero and the net force over the cross-section must be zero, i.e.

$$\sum_1^n A_j\sigma_j = 0 = \sum_1^n A_jE_j(\epsilon_j - \alpha_j T_j) \tag{1}$$

$$\sum_1^n A_j\sigma_j x_j = 0 = \sum_1^n A_jE_j x_j(\epsilon_j - \alpha_j T_j) \tag{2}$$

and

$$\sum_1^n A_j\sigma_j y_j = 0 = \sum_1^n A_jE_j y_j(\epsilon_j - \alpha_j T_j). \tag{3}$$

If it is assumed that plane sections remain plane, then

$$\epsilon_j = \epsilon_0 + px_j + qy_j \tag{4}$$

and substituting from (4) into (1) we obtain

$$\epsilon_0 \sum_1^n A_jE_j + p\sum_1^n A_jE_jx_j + q\sum_1^n A_jE_jy_j = \sum_1^n A_jE_j\alpha_j T_j. \tag{5}$$

If the origin of coordinates is chosen at the 'centroid' so that

$$\sum_1^n A_jE_jx_j = \sum_1^n A_jE_jy_j = 0 \tag{6}$$

then

$$\epsilon_0 = \frac{\sum_1^n A_jE_j\alpha_j T_j}{\sum_1^n A_jE_j}. \tag{7}$$

Substituting from (4) into (2), we obtain

$$\epsilon_0 \sum_1^n A_jE_jx_j + p\sum_1^n A_jE_jx_j^2 + q\sum_1^n A_jE_jx_jy_j = \sum_1^n A_jE_j\alpha_j T_jx_j. \tag{8}$$

If the axes of x and y are chosen to be principal axes so that

$$\sum_1^n A_j E_j x_j y_j = 0 \tag{9}$$

then

$$p = \frac{\sum_1^n A_j E_j \alpha_j T_j x_j}{\sum_1^n A_j E_j x_j^2} \tag{10}$$

and similarly

$$q = \frac{\sum_1^n A_j E_j \alpha_j T_j y_j}{\sum_1^n A_j E_j y_j^2} . \tag{11}$$

The equation for thermal stress then becomes

$$\sigma_j = E_j \left\{ \frac{\sum_1^n A_j E_j \alpha_j T_j}{\sum_1^n A_j E_j} + x_j \frac{\sum_1^n A_j E_j \alpha_j T_j x_j}{\sum_1^n A_j E_j x_j^2} + y_j \frac{\sum_1^n A_j E_j \alpha_j T_j y_j}{\sum_1^n A_j E_j y_j^2} - \alpha_j T_j \right\} . \tag{12}$$

The process of calculating the thermal stresses in a cooled blade requires detailed knowledge of the temperature distribution throughout the chordwise section of interest. The first steps in the calculation consist of dividing the blade section into a number of elements, assessing the mean temperature of each element and hence the appropriate value of Young's modulus. Then the x and y axes must be chosen to satisfy equations (6) and (9). With no variation of Young's modulus, this would mean simply that the origin of coordinates should be at the centroid of the blade section and that the x and y axes should be principal axes, such that the product of inertia, $\sum_1^n A_j x_j y_j$, is zero. The standard methods for finding principal axes are well known; all that need be emphasized here is that these calculations should be performed with care in order to permit a reliable method of checking subsequent stress calculations.

The flexural rigidity, $\sum_1^n A_j E_j x_j^2$, of the section about each principal axis must then be calculated. For each element the quantities $\alpha_j T_j$ and $A_j E_j \alpha_j T_j$ must be obtained, bearing in mind that the correct value of α_j is the mean value over the temperature rise T_j. Finally the summations $\sum_1^n A_j E_j \alpha_j T_j$, $\sum_1^n A_j E_j \alpha_j T_j x_j$, $\sum_1^n A_j E_j \alpha_j T_j y_j$ must be made. These can be inserted into equation (12) to provide a formula for the thermal stress at any point x_j, y_j where E_j, α_j and T_j are known.

It is worth noting that if $\sum_1^n A_j E_j x_j y_j = 0$, the relations (1), (2) and (3) can be used to check the accuracy of the calculation viz.

$$\sum_1^n \sigma_j A_j = \sum_1^n \sigma_j A_j x_j = \sum_1^n \sigma_j A_j y_j = 0 .$$

This arises because thermal stresses produce no resultant force or moment about a blade section. If for example (1) and (2) are satisfied but (3) is not, an error has occurred in the evaluation of q {equation (11)}.

APPENDIX III

Redistribution of Thermal Stress Due to Creep

At any point let the actual increase in strain during a given time interval be $\Delta\epsilon_j$. If the creep strain increase which occurs at this point in the same time interval is ΔC_j, then the stress change is given by

$$\Delta\sigma_j = E_j(\Delta\epsilon_j - \Delta C_j). \tag{1}$$

ΔC_j will depend on σ_j over the time interval and also on T_j.

Because there is no change in the loading of the specimen,

$$\sum_1^n A_j\Delta\sigma_j = \sum_1^n A_j\Delta\sigma_j x_j = \sum_1^n A_j\Delta\sigma_j y_j = 0. \tag{2}$$

If it is also assumed that plane sections remain plane, then

$$\Delta\epsilon_j = \Delta\epsilon_0 + lx_j + my_j. \tag{3}$$

Combining (1) and (3), applying the conditions of (2) in turn and again assuming that

$$\sum_1^n A_jE_jx_j = \sum_1^n A_jE_jy_j = \sum_1^n A_jE_jx_jy_j = 0 \tag{4}$$

we obtain

$$\Delta\epsilon_0 = \frac{\sum_1^n A_jE_j\Delta C_j}{\sum_1^n A_jE_j} \tag{5}$$

$$l = \frac{\sum_1^n A_jE_j\Delta C_jx_j}{\sum_1^n A_jE_jx_j^2} \tag{6}$$

$$m = \frac{\sum_1^n A_jE_j\Delta C_jy_j}{\sum_1^n A_jE_jy_j^2} \tag{7}$$

so that

$$\Delta\sigma_j = E_j\left\{\frac{\sum_1^n A_jE_j\Delta C_j}{\sum_1^n A_jE_j} + x_j\frac{\sum_1^n A_jE_j\Delta C_jx_j}{\sum_1^n A_jE_jx_j^2} + y_j\frac{\sum_1^n A_jE_j\Delta C_jy_j}{\sum_1^n A_jE_jy_j^2} - \Delta C_j\right\}. \tag{8}$$

The basic method for calculating stress changes over a given time interval is very similar in structure to that described in Appendix II for the calculation of thermal stresses. Instead of finding values of α_jT_j for each element, as in Appendix II, values of ΔC_j are needed. As previously stated ΔC_j will depend on σ_j over the time interval and also on T_j. In the stress-redistribution calculations

described in the main text, ΔC_j was taken to be equal to the increment of creep strain in a test specimen at T_j over the same interval of time as the one in question (e.g. 5 to 10 hr), and with a stress equal to that acting on the element at the beginning of the interval.

A more accurate solution would have been obtained by estimating the mean value of stress over the time interval in question and basing ΔC_j on that. This of necessity involves an iterative solution and can be avoided without serious loss of accuracy by taking sufficiently short time intervals.

Fortunately the calculation tends to compensate itself in that if the stress changes calculated for a given time interval are too large, the corresponding changes over the next interval will tend to be too small.

TABLE 1

Operating Conditions

Gas inlet total temperature	1500°K
Rotational speed	12 000 rev/min
Cooling-air flow supplied to the rotor blades (as a fraction of the main gas flow)	1·8 per cent
Cooling-air supply temperature	310°K

TABLE 2

Manufacturer's Data on Nimonic 90 *Material from which Blades Were Made*

Cast No.	Percentage chemical composition			Stress/rupture tests at 9 ton/in² and 870°C (life in hours)
	C	Ti	Al	
XH 296	0·05	2·55	1·24	39 } original batch
XH 200	0·06	2·48	1·36	51 } original batch
XH 341	0·08	2·28	1·29	63 } original batch
XJ 177	0·07	2·40	1·39	88 replacement batch

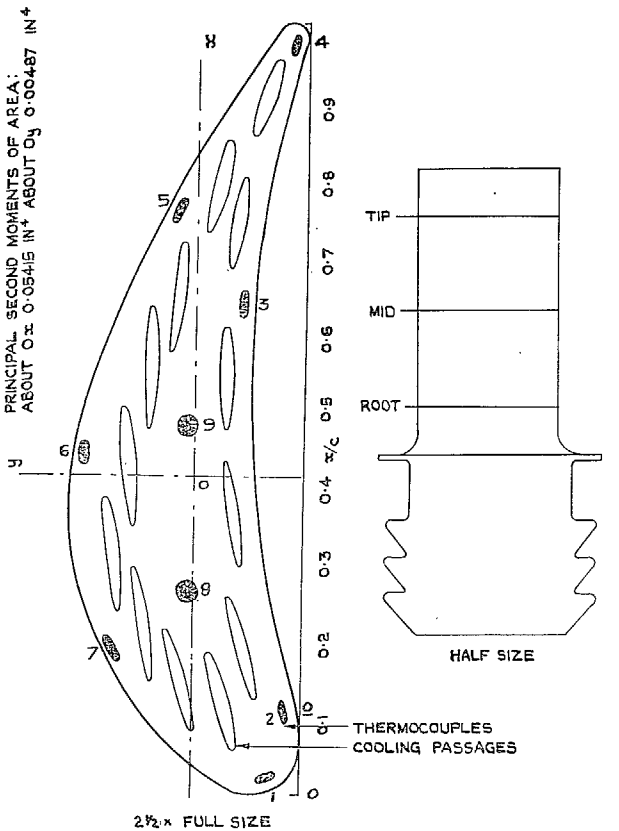

FIG. 1. Rotor blade showing thermocouple positions.

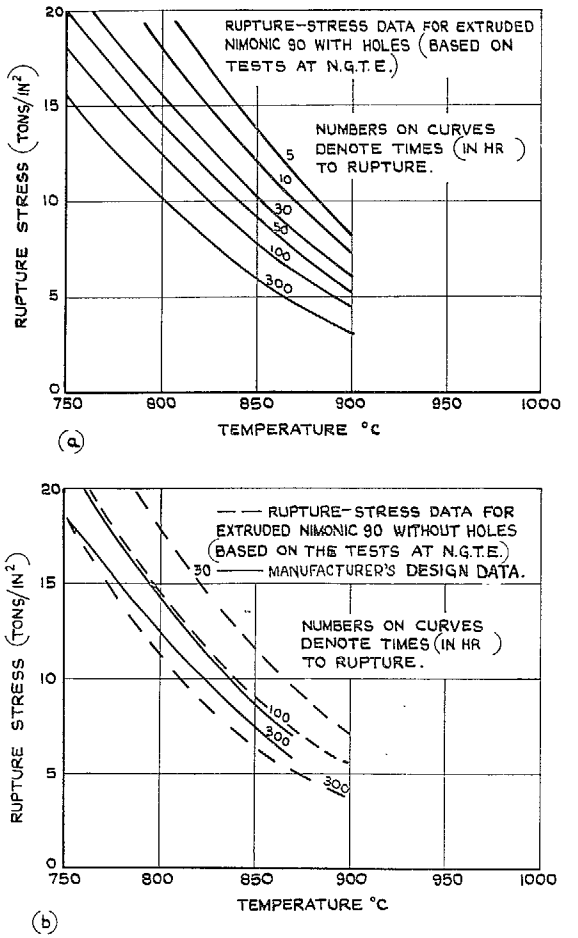

FIG. 2. Creep-rupture data for Nimonic 90.

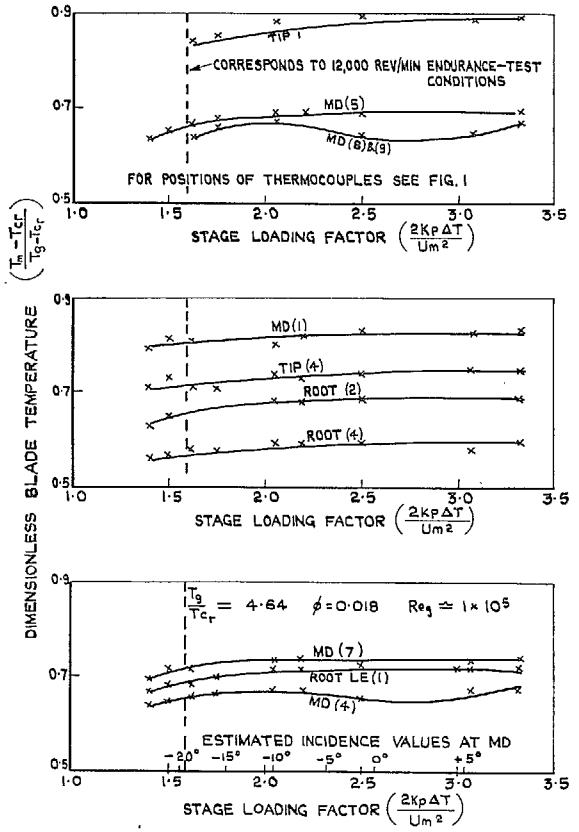

FIG. 3. Influence of aerodynamic stage loading on rotor-blade temperature measured on the 126 turbine.

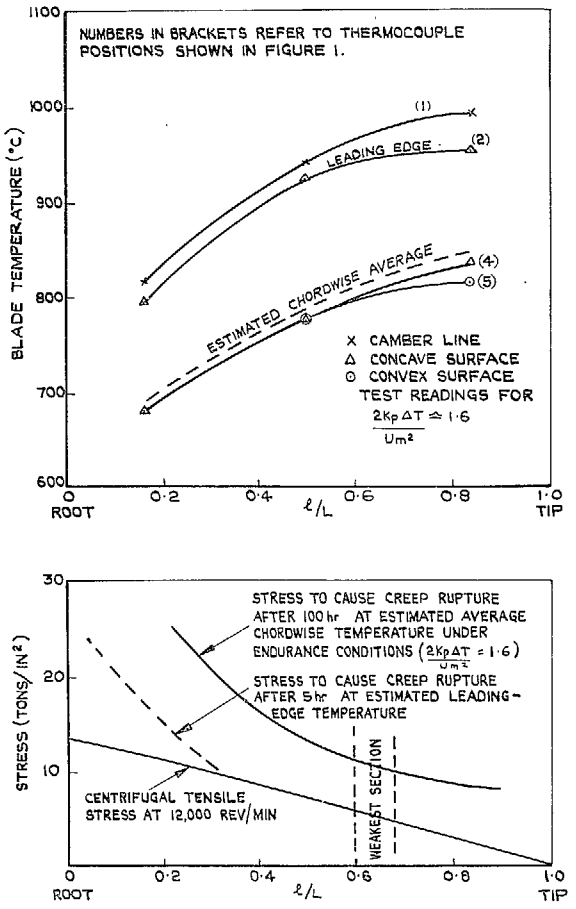

FIG. 4. Spanwise variations of temperature and stress for 126 turbine rotor blades under endurance-test conditions.

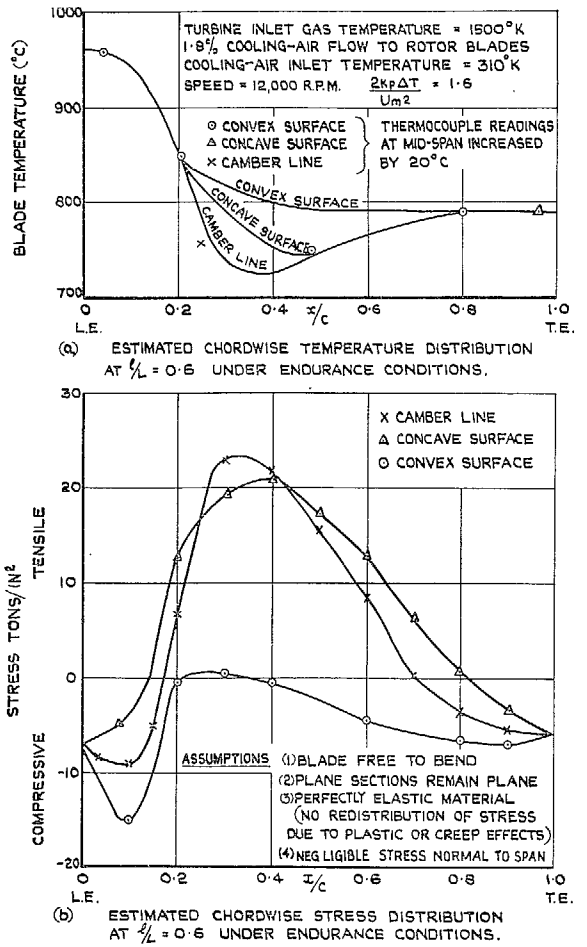

FIG. 5. Rotor-blade temperatures and stresses at 60% span.

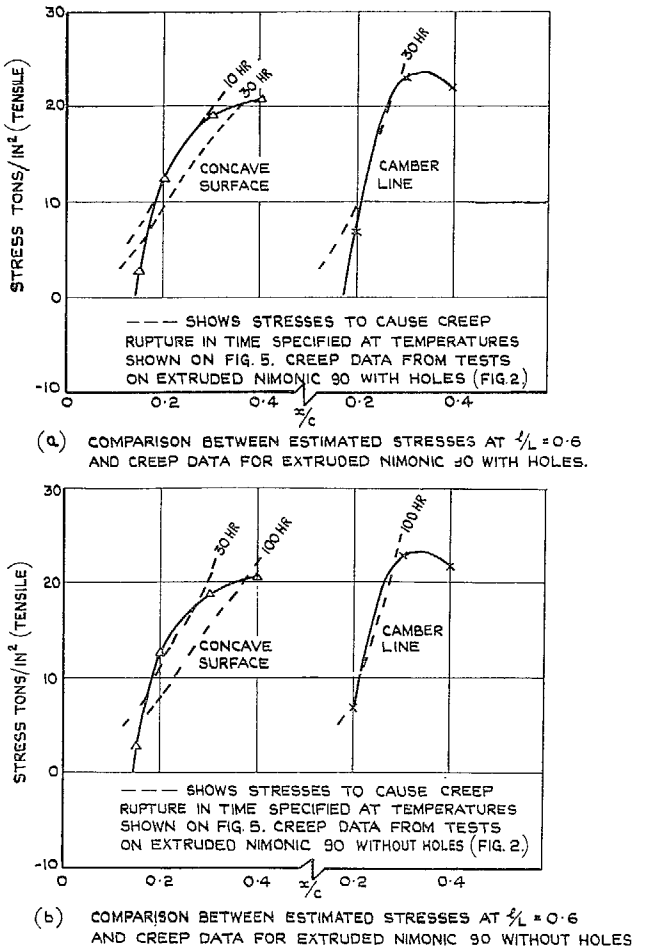

FIG. 6. Comparison between stresses and creep data.

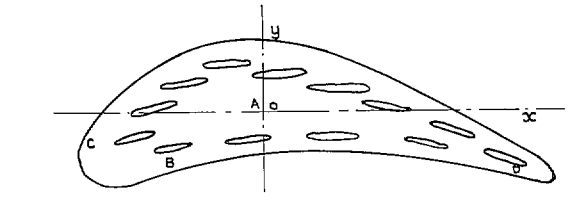

N.B.
IF STRESSES DID NOT REDISTRIBUTE WITH TIME CREEP DATA USED FOR THIS CALCULATION WOULD PREDICT FAILURE AT POSITION B (16·5 ton/in², 824°C) AFTER 30 HR WITH A CREEP STRAIN OF $4{\cdot}4 \times 10^{-2}$

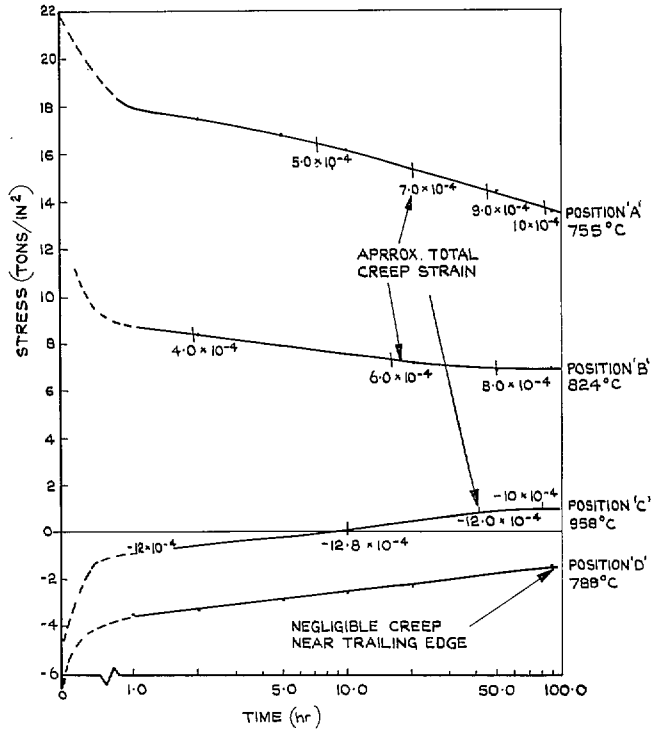

FIG. 7. Calculated stress redistribution at four chosen points ($l/L = 0{\cdot}6$).

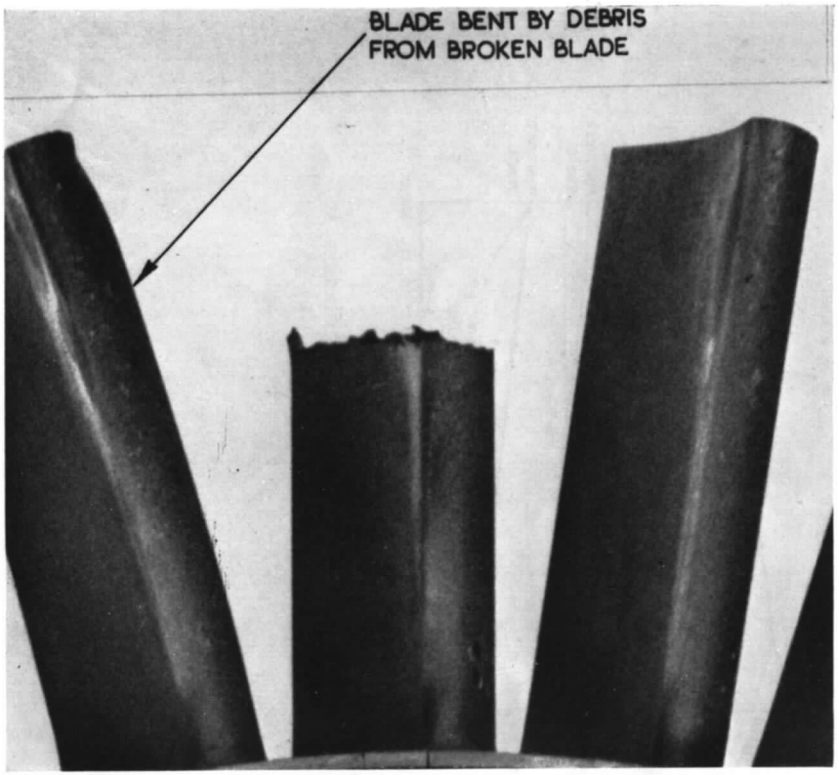

(a) Third broken blade showing fracture at approximately 60 per cent of span.

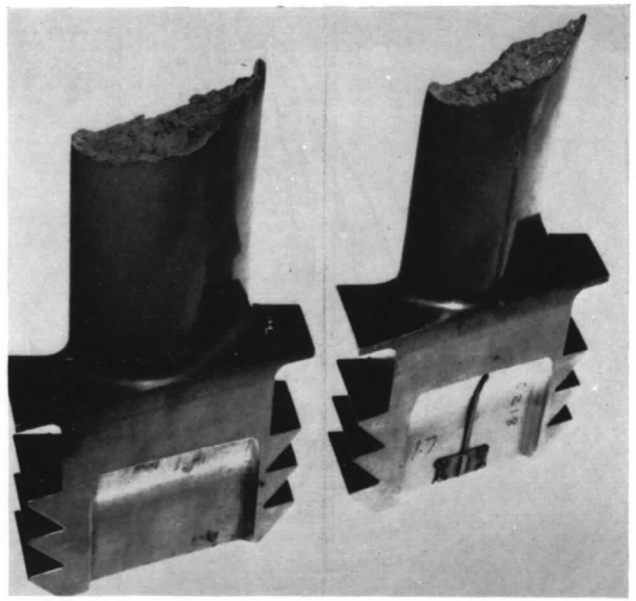

(b) Second and third broken blades showing similarity of fractures.

FIG. 8. Details of broken blades.

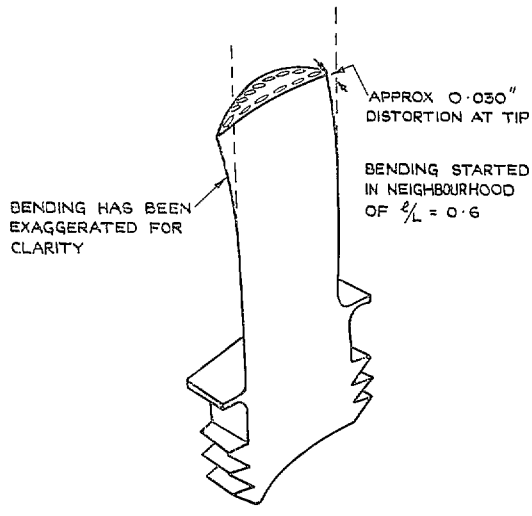

FIG. 9a. Sketch of bent blade showing distortion after 10 hours.

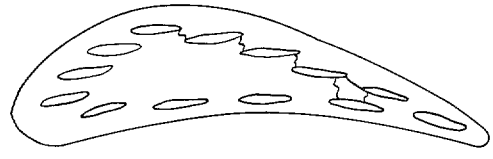

FIG. 9b. Spanwise cracks observed at root, mid-span and tip sections of bent blade.

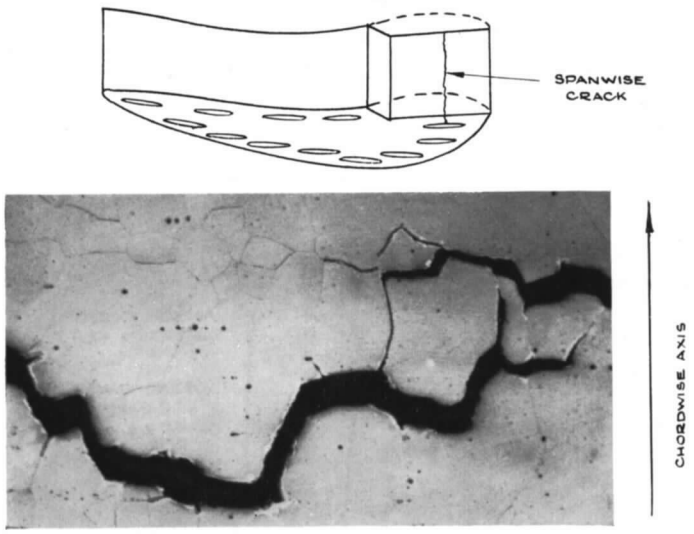

(a) Typical spanwise crack between cooling passages near leading edge (× 75).

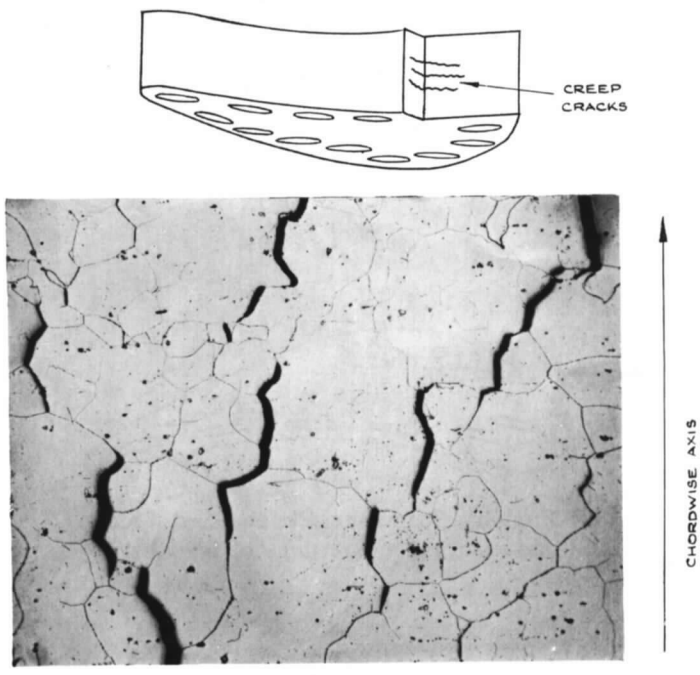

(b) Creep cracks near mid-span of bent blade (× 75).

FIG. 10. Photo-micrographs of cracking in rotor blades.

(91433) Wt. 66/2301 K.5 5/65 Hw.

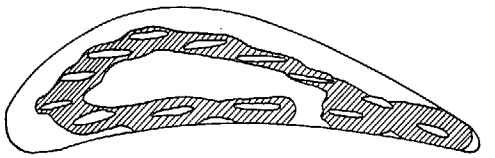

FIG. 11a. Typical disposition of coarse grains around cooling holes for original batch of material.

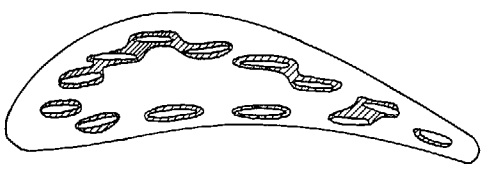

FIG. 11b. Typical disposition of coarse grains around cooling holes for replacement batch of material.

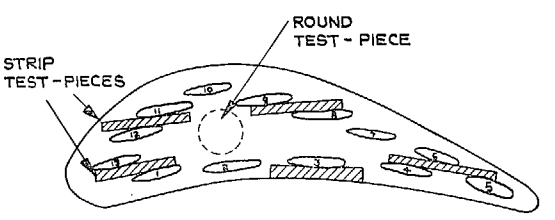

FIG. 11c. Positions of creep test-pieces.

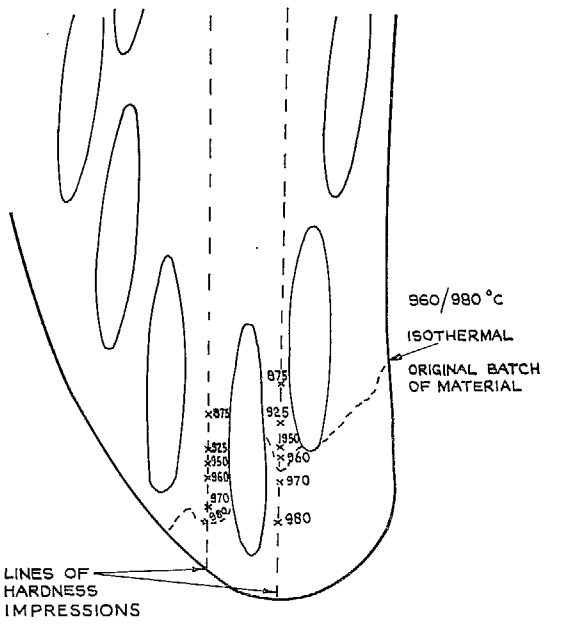

FIG. 12. Typical temperatures near leading edge at $l/L = 0{\cdot}75$ deduced from hardness measurements and structural changes.

Publications of the Aeronautical Research Council

ANNUAL TECHNICAL REPORTS OF THE AERONAUTICAL RESEARCH COUNCIL (BOUND VOLUMES)

1945 Vol. I. Aero and Hydrodynamics, Aerofoils. £6 10*s*. (£6 13*s*. 6*d*.)
Vol. II. Aircraft, Airscrews, Controls. £6 10*s*. (£6 13*s*. 6*d*.)
Vol. III. Flutter and Vibration, Instruments, Miscellaneous, Parachutes, Plates and Panels, Propulsion. £6 10*s*. (£6 13*s*. 6*d*.)
Vol. IV. Stability, Structures, Wind Tunnels, Wind Tunnel Technique. £6 10*s*. (£6 13*s*. 3*d*.)

1946 Vol. I. Accidents, Aerodynamics, Aerofoils and Hydrofoils. £8 8*s*. (£8 11*s*. 9*d*.)
Vol. II. Airscrews, Cabin Cooling, Chemical Hazards, Controls, Flames, Flutter, Helicopters, Instruments and Instrumentation, Interference, Jets, Miscellaneous, Parachutes. £8 8*s*. (£8 11*s*. 3*d*.)
Vol. III. Performance, Propulsion, Seaplanes, Stability, Structures, Wind Tunnels. £8 8*s*. (£8 11*s*. 6*d*.)

1947 Vol. I. Aerodynamics, Aerofoils, Aircraft. £8 8*s*. (£8 11*s*. 9*d*.)
Vol. II. Airscrews and Rotors, Controls, Flutter, Materials, Miscellaneous, Parachutes, Propulsion, Seaplanes, Stability, Structures, Take-off and Landing. £8 8*s*. (£8 11*s*. 9*d*.)

1948 Vol. I. Aerodynamics, Aerofoils, Aircraft, Airscrews, Controls, Flutter and Vibration, Helicopters, Instruments, Propulsion, Seaplane, Stability, Structures, Wind Tunnels. £6 10*s*. (£6 13*s*. 3*d*.)
Vol. II. Aerodynamics, Aerofoils, Aircraft, Airscrews, Controls, Flutter and Vibration, Helicopters, Instruments, Propulsion, Seaplane, Stability, Structures, Wind Tunnels. £5 10*s*. (£5 13*s*. 3*d*.)

1949 Vol. I. Aerodynamics, Aerofoils. £5 10*s*. (£5 13*s*. 3*d*.)
Vol. II. Aircraft, Controls, Flutter and Vibration, Helicopters, Instruments, Materials, Seaplanes, Structures, Wind Tunnels. £5 10*s*. (£5 13*s*.)

1950 Vol. I. Aerodynamics, Aerofoils, Aircraft. £5 12*s*. 6*d*. (£5 16*s*.)
Vol. II. Apparatus, Flutter and Vibration, Meteorology, Panels, Performance, Rotorcraft, Seaplanes. £4 (£4 3*s*.)
Vol. III. Stability and Control, Structures, Thermodynamics, Visual Aids, Wind Tunnels. £4 (£4 2*s*. 9*d*.)

1951 Vol. I. Aerodynamics, Aerofoils. £6 10*s*. (£6 13*s*. 3*d*.)
Vol. II. Compressors and Turbines, Flutter, Instruments, Mathematics, Ropes, Rotorcraft, Stability and Control, Structures, Wind Tunnels. £5 10*s*. (£5 13*s*. 3*d*.)

1952 Vol. I. Aerodynamics, Aerofoils. £8 8*s*. (£8 11*s*. 3*d*.)
Vol. II. Aircraft, Bodies, Compressors, Controls, Equipment, Flutter and Oscillation, Rotorcraft, Seaplanes, Structures. £5 10*s*. (£5 13*s*.)

1953 Vol. I. Aerodynamics, Aerofoils and Wings, Aircraft, Compressors and Turbines, Controls. £6 (£6 3*s*. 3*d*.)
Vol. II. Flutter and Oscillation, Gusts, Helicopters, Performance, Seaplanes, Stability, Structures, Thermodynamics, Turbulence. £5 5*s*. (£5 8*s*. 3*d*.)

1954 Aero and Hydrodynamics, Aerofoils, Arrester gear, Compressors and Turbines, Flutter, Materials, Performance, Rotorcraft, Stability and Control, Structures. £7 7*s*. (£7 10*s*. 6*d*.)

Special Volumes

Vol. I. Aero and Hydrodynamics, Aerofoils, Controls, Flutter, Kites, Parachutes, Performance, Propulsion, Stability. £6 6*s*. (£6 9*s*.)
Vol. II. Aero and Hydrodynamics, Aerofoils, Airscrews, Controls, Flutter, Materials, Miscellaneous, Parachutes, Propulsion, Stability, Structures. £7 7*s*. (£7 10*s*.)
Vol. III. Aero and Hydrodynamics, Aerofoils, Airscrews, Controls, Flutter, Kites, Miscellaneous, Parachutes, Propulsion, Seaplanes, Stability, Structures, Test Equipment. £9 9*s*. (£9 12*s*. 9*d*.)

Reviews of the Aeronautical Research Council

1949–54 5*s*. (5*s*. 5*d*.)

Index to all Reports and Memoranda published in the Annual Technical Reports

1909–1947 R. & M. 2600 (out of print)

Indexes to the Reports and Memoranda of the Aeronautical Research Council

Between Nos. 2451–2549: R. & M. No. 2550 2*s*. 6*d*. (2*s*. 9*d*.); Between Nos. 2651–2749: R. & M. No. 2750 2*s*. 6*d*. (2*s*. 9*d*.); Between Nos. 2751–2849: R. & M. No. 2850 2*s*. 6*d*. (2*s*. 9*d*.); Between Nos. 2851–2949: R. & M. No. 2950 3*s*. (3*s*. 3*d*.); Between Nos. 2951–3049: R. & M. No. 3050 3*s*. 6*d*. (3*s*. 9*d*.); Between Nos. 3051–3149: R. & M. No. 3150 3*s*. 6*d*. (3*s*. 9*d*.); Between Nos. 3151–3249: R. & M. No. 3250 3*s*. 6*d*. (3*s*. 9*d*.); Between Nos. 3251–3349: R. & M. No. 3350 3*s*. 6*d*. (3*s*. 10*d*.)

Prices in brackets include postage

Government publications can be purchased over the counter or by post from the Government Bookshops in London, Edinburgh, Cardiff, Belfast, Manchester, Birmingham and Bristol, or through any bookseller

Printed and published by
HER MAJESTY'S STATIONERY OFFICE

To be purchased from
York House, Kingsway, London W.C.2
423 Oxford Street, London W.1
13A Castle Street, Edinburgh 2
109 St. Mary Street, Cardiff
39 King Street, Manchester 2
50 Fairfax Street, Bristol 1
35 Smallbrook, Ringway, Birmingham 5
80 Chichester Street, Belfast 1
or through any bookseller

Printed in England

S.O. Code No. 23-3404